

1 **Macrozooplankton and micronekton diversity and associated carbon**
2 **vertical patterns and fluxes under distinct productive conditions around**
3 **the Kerguelen Islands**

4
5
6
7 Cotté C.^{1,*}, Berne A.^{1,2}, Habasque J.², Lebourges-Dhaussy A.², Roudaut G.², Espinasse B.³, Hunt
8 B.P.V.^{4,5,6}, Pakhomov E.A.^{4,5,6}, Henschke N.⁴, Peron C.⁷, Conchon A.¹, Koedooder C.^{8,9}, Ariza A.¹⁰,
9 Cherel Y.¹¹

10
11
12
13 ¹Sorbonne Université, CNRS, IRD, MNHN, Laboratoire d’Océanographie et du Climat:
14 Expérimentations et Approches Numériques (LOCEAN-IPSL), Paris, France

15 ²LEMAR, UBO-CNRS-IRD-Ifremer IUEM, Plouzané, France

16 ³Department of Arctic and Marine Biology, UiT The Arctic University of Norway, Tromsø, Norway.

17 ⁴Department of Earth, Ocean and Atmospheric Sciences, University of British Columbia, Vancouver,
18 British Columbia, Canada

19 ⁵Institute for the Oceans and Fisheries, University of British Columbia, Vancouver, British Columbia,
20 Canada

21 ⁶Hakai Institute, PO Box 309, Heriot Bay, BC, Canada

22 ⁷BOREA, MNHN- CNRS-UPMC-IRD-UCBN-UAG, Paris, France

23 ⁸Sorbonne Université, UPMC Univ Paris 06, CNRS, Laboratoire d’Océanographie Microbienne
24 (LOMIC), Observatoire Océanologique, Banyuls/mer, France.

25 ⁹The Fredy and Nadine Herrmann Institute of Earth Sciences, Hebrew University of Jerusalem,
26 Jerusalem, Israel.

27 ¹⁰MARBEC, Univ. Montpellier, CNRS, Ifremer, IRD, Sète, France

28 ¹¹Centre d’Etudes Biologiques de Chizé (CEBC), UMR 7372 du CNRS-La Rochelle Université, 79360
29 Villiers-en-Bois, France

30
31 *Corresponding author: cedric.cotte@locean.ipsl.fr

32 **Abstract**

33

34 Mesopelagic communities are characterized by a large biomass of diverse macrozooplankton and
35 micronekton (MM) performing diel vertical migration (DVM) connecting the surface to the deeper
36 ocean and contributing to biogeochemical fluxes. In the Southern Ocean, a largely High Nutrient Low
37 Chlorophyll (HNLC) and low carbon export region, the contribution of MM to the vertical carbon flux
38 of the biological pump remains largely unknown. Furthermore, few studies have investigated MM
39 communities and vertical flux in naturally iron fertilized areas associated with shallow bathymetry. In
40 this study we assessed the MM community diversity, abundance and biomass in the Kerguelen Island
41 region, including two stations in the HNLC region upstream of the islands, and two stations in naturally
42 iron fertilized, one on the plateau, and one downstream of the plateau. The MM community was
43 examined using a combination of trawl sampling and acoustic measurements at 18 and 38 kHz from the
44 surface to 800m. A conspicuous vertical three-layers system was observed at all four stations: a shallow
45 scattering layer (SSL, between 10 and 200 m), mid-depth scattering layers (MSL, between 200 and 500
46 m) and deep scattering layers (DSL, between 500 and 800 m). While salps (*Salpa thompsoni*)
47 dominated the biomass at the productive Kerguelen plateau and the downstream station, they were
48 scarce at the HNLC stations upstream of the islands. In addition, crustaceans (mainly *Euphausia*
49 *vallentini* and *Themisto gaudichaudii*) were particularly abundant over the plateau, representing a large,
50 although varying, carbon stock in the 0-500 m water layer. Mesopelagic fish were prominent below
51 500m where they formed permanent or migrant layers accounting for the main source of carbon.
52 Through these spatial and temporal sources of variability, complex patterns of the MM vertical
53 distribution and associated carbon content were identified. The respiratory carbon flux mediated by
54 migratory myctophids at the four stations was quantified and evaluated for possible inaccuracies. While
55 the estimated levels are likely underestimated, this study highlights the importance of migrant biomass
56 and size structure in the biological pump of the Southern Ocean regions affected by complex
57 topography and land mass effects..

58

59

60 **Keywords:** macrozooplankton; micronekton; vertical patterns; migratory flux; spatio-temporal
61 variability; acoustic; Kerguelen plateau; Southern ocean

62 **Introduction**

63 The mesopelagic community is composed of taxonomically and functionally diverse groups of
64 organisms, including gelatinous organisms, crustaceans and mesopelagic fish, that occupy the 200-
65 1000 m depth zone in the ocean. Through modelling and *in-situ* studies, mesopelagic organisms have
66 gained an increasing attention from the ecological and biogeochemical communities (Davison et al.,
67 2013, Anderson et al., 2018, Hernández-León et al., 2019) as well as from managers interested in the
68 sustainable exploitation of potential new resources. This interest has primarily been stimulated by two
69 characteristics of the mesopelagic zooplankton and micronekton. First, while logistical and
70 technological difficulties in reliably estimating zooplankton and fish biomass still exist, recent
71 assessments have pointed to a high likelihood of these populations being substantially underestimated
72 (Irigoién et al., 2014, Hernández-León et al., 2020). Secondly, mesopelagic organisms are known to
73 perform intensive diel vertical migration (DVM), described as the largest animal migration on Earth
74 (Hays, Sutton). This DVM connects the mesopelagic zone (200-1000 m) where mesopelagic organisms
75 reside during daytime to the surface epipelagic waters (0-200 m) which they move up to for feeding at
76 night. This vertical movement represents an important active contribution in the downward particle
77 export, and particularly the transport of carbon (Bianchi et al., 2013, Ariza et al., 2015).

78
79 The Southern Ocean is the world ocean's largest high nutrient low chlorophyll (HNLC) area where the
80 production is mainly limited by iron (de Baar et al., 1995). Naturally iron-fertilized sites generate
81 highly productive regions in the Southern Ocean (Blain et al., 2007). The Kerguelen Plateau forms a
82 large physical barrier to the eastward flowing Antarctic Circumpolar Current (ACC) and induces iron
83 enrichment of shelf waters that are then entrained in the downstream area eastward of the AAC flux
84 (Blain et al., 2007, Mongin et al., 2008). While upstream waters approaching the Kerguelen Islands are
85 generally depleted in iron and chlorophyll (Jandel et al., 1998), a large bloom occurs over the
86 Kerguelen plateau as well as in the downstream region, observed as a persistent and dynamical high-
87 chlorophyll plume (d'Ovidio et al., 2015). An inverse relationship has been observed between
88 production and export in this region, a typical feature of the Southern ocean (Maiti et al., 2013, Le
89 Moigne et al., 2016). However, to date only passive export has been considered in this region, and the
90 contribution of active carbon flux remains to be resolved. Given the prominent role of the Southern
91 Ocean in the global carbon cycle, estimates of active carbon flux are important to consider with respect
92 to the global carbon budget and it is fundamental to assess the contribution of the biological active
93 community of mesopelagic organisms. A need to improve the knowledge on their role in ecosystems,

94 including the diversity and their contribution in biogeochemical stocks and flux, has recently been
95 stressed (Ratnarajah et al., 2020, Martin et al., 2020).

96

97 The Kerguelen area offers an ideal location to investigate the functioning of the pelagic ecosystem,
98 including the biological pump, in contrasting production regimes with and without natural iron
99 enhancement.. This region is also ecologically important as a foraging ground for several species of
100 land-based marine top predators (Hindell et al., 2011). Their diet is largely comprised of
101 macrozooplankton and micronekton (MM) and the estimated food consumption by the highest trophic
102 level predators indicates the presence of a significant standing stock of mesopelagic micronekton,
103 primarily myctophids, and macrozooplankton, including euphausiids and hyperiids (Guinet et al., 1996,
104 Bocher et al., 2001, Bost et al., 2002, Cherel et al., 2002, Lea et al., 2002, Cherel et al., 2008). In this
105 subantarctic area of the Southern Ocean, high abundances of intermediate trophic levels have been
106 reported in association with either circumpolar frontal regions or local bathymetry-driven features
107 (Pakhomov et al., 1994, Pakhomov and Froneman 1999, Behagle et al., 2017). For instance, the
108 abundance of the subantarctic krill *Euphausia vallentini* was associated with the shelf topography and
109 the location of the Polar Front, and it was reported to be more numerous in the eastern area than the
110 western part of the Kerguelen region (Koubbi et al., 2011, Hunt et al., 2011). It has recently been
111 reported that, on a global scale, zooplankton biomass in the whole water column increases with the
112 average net primary production, implying an enhanced active export of carbon coupling the surface and
113 deep layers (Hernández-León et al., 2020).

114

115 The comparative approach used in this study, targeting iron fertilized vs HNLC sites, originated from
116 the scientific strategy of the KEOPS 1 and 2 campaigns (Queguiner et al., 2011). The objective of this
117 study was to understand how mid-trophic level MM respond to contrasting production regimes
118 (oligotrophic vs biologically-enriched zones). Specifically, we tested the hypothesis that high primary
119 production implies high diversity and/or high abundance of MM. Deployment of midwater trawls
120 allowed us to estimate the depth-stratified carbon content contributions of different taxonomic groups
121 and qualitatively assess their contributions to the active carbon flux in the area. Quantitatively, the
122 importance of mesopelagic fish to the active carbon transport was estimated using a recent compilation
123 of myctophid respiration rates in the Southern Ocean (Belcher et al., 2019). Species composition and
124 distribution patterns, including the derived fluxes, of MM from trawl data collections were
125 supplemented with acoustic backscatter analyses. The temporal monitoring of acoustic densities using

126 high-resolution measurements from the surface to 800 m appeared to be a powerful tool to assess the
127 complex and diverse vertical patterns between the different areas of interests in the Kerguelen region.

128 **Methods**

129 **- Survey**

130 The Mobydick survey (DOI: <https://doi.org/10.17600/18000403>) was carried out in the area south of
131 the Kerguelen Islands onboard the *R/V Marion Dufresne II*. From the 26th of February to the 19th of
132 March 2018, hydrographic and acoustic data, as well as MM samples were collected at four stations
133 (M1, M2, M3 and M4, Fig. 1). These stations were located based on knowledge from previous
134 oceanographic cruises conducted in the area (e.g., Blain et al., 2007, d'Ovidio et al., 2015, Behagle et
135 al., 2017). The M1 station was located east of the plateau in the area identified as the core foraging area
136 of the king penguin, an important top predator in terms of consuming biomass (Scheffer et al., 2016).
137 The M2 station located on the plateau (isobath 520m) corresponded to a reference station to study the
138 naturally fertilised bloom on the Kerguelen plateau (Quéguiner et al. 2011). The stations M3 and M4 to
139 the west of the plateau were chosen because HNLC conditions prevailed. While M1 was visited once,
140 M4 was visited twice and M2 thrice. The first visit of the M3 station with a full sampling of all depths
141 during daytime and nighttime was divided into two periods because of bad weather condition, so that
142 M3-1 and M3-2 were separated by an 11-day period.

143

144 **- Remote and in-situ oceanographic measurements**

145 Hydrological casts were carried out at each visit of all stations (Fig. 1). Temperature and chlorophyll *a*
146 concentration (Chl *a*) profiles were collected using SeaBird probes.

147 Sea surface chlorophyll data from Global Ocean Color products with a 1/24° resolution (from the
148 Marine Copernicus data portal) was used to build time series of Chl *a* at each station. We considered
149 the weekly averaged product (7 days) to describe the bloom temporal patterns since it represents a good
150 compromise between the temporal resolution and the cloud coverage. We also estimated the Polar Front
151 (PF) mean location in the Kerguelen area by using T and S profiles from the Global Ocean Reanalysis
152 (Ferry et al., 2016), as described in Pauthenet et al., (2018).

153

154 **- Acoustic measurements**

155 Continuous acoustic measurements were made with a calibrated (Demer et al., 2015, Simrad EK80
156 documentation) Simrad EK80 echosounder operating at five frequencies: 18, 38, 70, 120 and 200 kHz.
157 As we were interested to described acoustic scattering in epipelagic and mesopelagic waters, we only
158 used the 18 and 38 kHz frequencies, with maximum acquisition ranges of 1000 and 800 m respectively.

159 Data used in this study were acquired with an average ping interval of 3 s, mostly during station time
160 where the vessel was either immobile, or during trawling activity. See Table 1 for echosounder settings.
161 The acoustic data were scrutinized, corrected and analysed using the “Movies3D” software developed
162 at the “Institut Français de Recherche pour l'Exploitation de la Mer” (Ifremer; Trenkel et al., 2009)
163 combined with the French “Institut de Recherche pour le Développement” (IRD) open source tool
164 “Matecho” (Perrot et al., 2018), developed in MATLAB.

165 The noise from the surface (3 m deep from the transducer, that is 12 m deep from the surface) and the
166 bottom ghost echoes were excluded and the bottom line was corrected. Single-ping interferences from
167 electrical noise or other acoustic instruments (Le Bouffant, N., *comm. pers.*), and periods with either
168 noise or attenuated signal due to inclement weather, were removed using the filters described by Ryan
169 et al. (2015). Background noise was estimated and subtracted using methods described by De Robertis
170 and Higginbottom (2007). The nautical area scattering coefficient (NASC in $\text{m}^2 \text{nmi}^{-2}$), an indicator of
171 marine organisms biomass, and the volume backscattering strength (S_v in $\text{dB re } 1\text{m}^{-1}$), an indicator of
172 the marine organisms' density, were calculated. Acoustic symbols and units used here follow
173 MacLennan et al. (2002). Data were echo-integrated onto 0.5 m high layers over a 3 pings period
174 giving one ESU (Elementary Sampling Unit) with a -100 dB threshold from 12 m down to 800 m
175 depth.

176 The DVM is a common behaviour for zooplankton and micronekton that can be perceived at almost all
177 spatial scales (Haury et al., 1978). Acoustic data were thus split into day, night and crepuscular periods
178 (dawn and dusk). Day and night periods were defined based on the solar elevation angle with day when
179 the altitude is $>18^\circ$ and night with altitude $<-18^\circ$ (as in Lehodey et al., 2014).

180 Acoustic data were also spatially split between stations by creating a 0.8° Longitude 0.5° Latitude
181 rectangle around the GPS coordinate of each station (Fig. 1, blue rectangles). These rectangular areas at
182 each station encompass the trawl operations area. Acoustic data recorded during transits (i.e. out of
183 these spatial limits) were excluded from data analysis. The vertical profiles of mean acoustic density
184 NASC were computed for each visit of each station for the daytime and nighttime periods (not only
185 trawling time).

186

187 *Data visualisation-* Red Green Blue (RGB) composite images were generated in MATLAB based on
188 the 18 and 38 kHz echo-integrated acoustic data as in Annasawmy et al. (2019). The acoustic volume
189 backscattering strength S_v of the 18 kHz frequency was colour-coded in red while the 38 kHz was
190 displayed in colder hue using both blue and green, with a high threshold scale of -60 dB and a low
191 scale threshold of -90 dB. In the RGB composite image subsequently created, the hue gives the

192 frequency with the highest backscatter and the luminance gives the intensity of the volume
193 backscattering strength. A light cyan (combination of blue and green) colour indicates a dominant and
194 high 38 kHz backscatter whereas a dark red colour indicates a dominant but low 18 kHz backscatter. A
195 black hue indicates that all backscatters are under the low scale threshold or that no data are available,
196 and a white hue indicates that all backscatters are above the high threshold scale. Using these two
197 frequencies, the RGB echogram gave for each station, a clear and synthetic visual representation of the
198 location and migration in the water column of acoustic communities of scatterers based on their most
199 resonant frequency from 20 to 800 m.

200

201 - **Trawling**

202 Forty-eight trawls were performed, consisting of three night trawls and three day trawls at each station
203 (Table 2). Macrozooplankton and micronekton (MM) were collected during daytime and nighttime
204 using a Mesopelagos trawl, designed by Ifremer (fisheries biology and technology laboratory, LTBH,
205 Lorient, France) (Meillat, 2012). This trawl has a 7 m mean vertical opening and 12 m horizontal
206 opening, with a 65 m² mouth area and 44 m length. The trawl has a mesh size of 30 mm in the wings,
207 reducing to 4 mm in the codend. Trawl depth was monitored in real time with a Scanmar
208 (Åsgårdstrand, Norway) depth sensor attached to the trawl headline. We adopted a semi-
209 stratified/adaptive strategy in trawl sampling. As the aim was to provide the most complete picture of
210 the micronekton community at each station, the whole water column from the surface to 650 m was
211 sampled at different strata corresponding to the sound scattering layers at different depths: the shallow
212 scattering layers (SSL, between 10 and 200 m), the mid-depth scattering layers (MSL, between 200 and
213 500 m) and the deep scattering layers (DSL, between 500 and 800 m). At each layer, hauls were
214 performed at targeted depths according to the observations of the different scattering structures (patches
215 or layers) provided by the echosounders. The towing speed was maintained near 2 knots, with effective
216 fishing times of 30 minutes.

217 Once on board, the total wet mass (WM) in grams was weighed. Organisms were firstly sorted into
218 broad taxonomic groups (fish, crustaceans, gelatinous organisms and cephalopods), then identified at
219 the species level. All organisms were counted and weighed; fish and salps were also measured.

220 The allocated temperature estimate for each trawl was performed by using the temperature profile from
221 the CTD cast closest to the trawl location in space and time, and by taking the estimated temperature at
222 the trawl depth (during the fishing period).

223

224 - **Estimates of C content**

225 Carbon biomass was estimated using conversion factors to convert WM in dry mass (DM) and DM in
226 carbon biomass for the four main taxonomic groups, gelatinous organisms, fish, molluscs and
227 crustaceans. Water content for each of the group was estimated based on available data from the
228 literature as follow: 94% for gelatinous organisms (Larson 1986, Huntley et al 1989), 75% and 80% for
229 fish and molluscs, respectively, (Schaafsma et al., 2018) and 75% for crustaceans (Schaafsma et al.,
230 2018, Harris et al., 2000). The carbon content of dry biomass was provided in the context of stable
231 isotopes analysis (Hunt et al., this issue) carried out on all the main taxa. The percentage of C in DM
232 was then averaged for each group such as gelatinous organisms 15%, fish 50%, molluscs 35% and
233 crustaceans 40%.

234

235 - **Migrant biomass and carbon flux**

236 Additionally, biomass and carbon flux were estimated for migratory fish of the family Myctophidae.
237 This group was targeted as migratory layers found at night near surface, and more importantly, because
238 it was possible to estimate carbon flux using metabolic predictive equations specifically developed for
239 this family (Belcher et al., 2019).

240 We assumed that all myctophids found at nighttime in the epipelagic layer would return to the
241 mesopelagic at day. Migration was then calculated as the abundance and biomass of myctophids in the
242 nocturnal shallow trawls 5, 6, 11, 19, 20, 21, 31, 35, 37, 39, and 48. This was standardized for the
243 volume filtered by the net, and it was integrated by the thickness of the sound scattering layer (from
244 echograms) where net was located. Abundance and biomass was expressed as the number of
245 individuals or the milligrams of carbon weight by square metre (ind m^{-2} , mg C m^{-2}).

246

247 Carbon flux mediated by respiration was estimated by calculating the amount of carbon dioxide
248 exhaled by myctophids below the thermocline. For this, the respiration rate for each individual was
249 estimated using body mass and environmental temperature as predictors, following the respiration
250 regression developed for myctophid fish in Belcher et al. (2019):

251

$$252 \quad \text{Ln}(R_{WM}) = -1.315 - 0.2665 \times \text{Ln}(WM) + 0.0848 \times T \quad \text{Eq. 1}$$

253

254 where R_{WM} is the mass-specific respiration rate per hour ($\mu\text{l O}_2 \text{ mg WM}^{-1} \text{ h}^{-1}$), WM is the individual
255 wet mass (mg), and T is the environmental temperature ($^{\circ}\text{C}$). Individual wet mass was estimated using
256 the length-weight relationships provided for the family Myctophidae by Kwong et al. (2020).

257 Respiration was computed for 2.2 $^{\circ}\text{C}$, corresponding to the average temperature in waters between 400

258 and 500 m depth. This interval was assumed as the end of migration, according to the daytime migrant
259 layer depth registered with the echosounder. The total respiration for each trawl was calculated by
260 standardising the volume filtered by the net (considering a cylinder with the surface of the trawl
261 opening and the distance traveled during the haul), and summing for all myctophid individuals captured
262 in that trawl. Similarly to the abundance and biomass measurements, total respiration was integrated by
263 the thickness of the sound scattering layer where net was located. This was then converted to units of
264 carbon per square meter and day ($\text{mg C m}^{-2} \text{ d}^{-1}$) using a respiratory quotient of 0.90 for fishes (Brett
265 and Groves, 1979, Ariza et al., 2015) and the stoichiometric relationship between carbon and oxygen
266 ($22.4 \text{ L O}_2 = 12 \text{ g carbon}$). Since carbon export to the mesopelagic zone only occur during daytime,
267 only 12 hours of the day were considered for calculations.

268 **Results**

269 **- Environmental conditions around Kerguelen plateau**

270 In addition to their location relative to the plateau (on the plateau vs upstream/downstream areas), the
271 stations were also situated within the area of a particular oceanographic feature, the PF, which crossed
272 the plateau just south of the Kerguelen Islands (Fig. 1). The M1, M2 and M4 stations were located
273 south of the PF, with varying distances to the PF mean location, while the M3 station was located north
274 of this front.

275 During the cruise, the concentration of Chl *a* was higher at station M2 on the plateau compared to the
276 downstream and upstream stations (Fig. 2). Overall, the concentrations (both over and outside the
277 plateau) during the survey were considered low ($<0.4 \text{ mg}\cdot\text{m}^{-3}$) compared to the concentrations observed
278 during the spring/summer period from October to January. Throughout this period, the highest Chl *a*
279 was measured on the plateau in mid-January. Medium values occurred upstream (M3 and M4) with a
280 simultaneous peak. An earlier (late November) maximum was observed downstream.

281

282 **- Description of the macrozooplankton/micronekton community from trawl collection.**

283 Over the whole study area, the dominant biomass obtained from the trawl samples was attributed to
284 gelatinous organisms (Fig. 3). In most trawls, they constituted a major part of the absolute biomass, i.e.
285 an average weight per sample of 3497 g (± 7837 g) corresponding to a mean proportion of 63 %
286 (± 33.35 %) of the total weight (Fig. 4). This was followed by crustaceans, with an average weight per
287 sample of 312 g (± 275 g) corresponding to a mean proportion of 30 % (± 31 %), and fish with an
288 average weight per sample of 133 g (± 193 g) corresponding to a mean proportion of 6.5 % (± 10.4 %).
289 In trawls with a low total biomass (<1000 g), the gelatinous dominance was challenged by a higher
290 relative biomass of crustaceans (Fig. 4), particularly for samples carried out during daytime at depths
291 shallower than 300 m. This trend was supported by the high relative abundance of crustaceans, which
292 contributed more than half of the total organisms in 75 % of the 48 trawls (Fig. 5).

293 In terms of biomass, the most important gelatinous contributors were salps (*Salpa thompsoni*) followed
294 by siphonophores (especially *Rosacea plicata*) (Fig. 6 and Table 3). Notably, *S. thompsoni* was only
295 abundant at stations M1 and M2. Chaetognathes were also often found in trawls with a relatively low
296 biomass. Ctenophores (*Bolinopsis* sp.) and jellyfish (mostly scyphozoans) contributed variably in the
297 proportion of gelatinous organisms with species occurring in half of the trawls (e.g., *Calycopepis*
298 *borchgrevinki*) and contributing weakly to moderately to biomass (such as *Atolla wyvillei* and
299 *Periphylla periphylla*).

300 For crustaceans, the most common species in terms of occurrence and abundance were the euphausiid
301 *E. vallentini* and the hyperiid amphipod *Themisto gaudichaudii* (Fig. 7 and Table 4). The latter was the
302 only species among all taxonomic groups found in all trawls, but it was particularly abundant at M2
303 over the shelf. The euphausiid *Euphausia triacantha* was also frequently found, though with a lower
304 abundance than *E. vallentini*. Other hyperiid amphipods, e.g. *Cylopus magellanicus* and *Primno*
305 *macropa*, often occurred in trawls albeit at relatively low abundances.

306 The dominant fish family was Myctophidae with 3367 individuals belonging to 14 species (Fig. 8 for
307 myctophids only, Table 5 and supplemental material 1 for the main fish species). The most abundant
308 species within the whole fish community was *Krefflichthys anderssoni*, which represents half of the
309 fish caught when merging adults and post-larvae. *Electrona antarctica* was also an abundant species
310 and the most frequent fish in all trawls. Other myctophids, such as *Gymnoscopelus braueri* and
311 *Protomyctophum bolini* had a high occurrence but were low to moderately abundant. Other fish
312 families were characterized by either a high occurrence (i.e., *Notolepis coatsi*) or locally a high
313 abundance (e.g., *Bathylagus tenuis*, *Cyclothone* sp.).

314 315 - Variability in vertical patterns from acoustic and trawl records

316 -Diel variability-

317 **Diel variability in biomass and acoustic densities:** A strong variability was observed in the vertical
318 distribution of both biomass and acoustic densities between nighttime and daytime. Very low biomass
319 was sampled in the SSL during daytime (Fig. 3). However, acoustic profiles indicated that densities,
320 organized in relatively thin peaks, occurred in this layer at ~100 m depth during both nighttime and
321 daytime (Fig. 9). At depth, diel differences regarding biomass was less clear and acoustic densities was
322 variable. Recurrent medium densities were observed between 400-500 m during daytime and between
323 250-400 m during night-time. The 38 kHz backscatter is globally lower than the 18kHz between the
324 surface and 500 m, while an opposite pattern occurred at depths >500 m. Despite acoustic structures
325 moved vertically between daytime and nighttime and variable patches and layers were observed in the
326 RGB echograms, a conspicuous 3-layers system characterized the whole area (Fig. 10). During
327 daytime, clear scattering layers appeared and various patches were observed whereas acoustic
328 scattering features were more consistent in the horizontal axis. Transition periods (dusk and dawn)
329 evidenced different patterns of vertical migrations between the surface and the underlying deeper
330 layers, including vertical movements deeper than 800 m. Migratory organisms were more responsive at
331 18kHz, while a permanent non-migratory layer was observed at 600 m, which was characterized by an
332 intense 38kHz signal (in dB).

333

334 **Diel variability in communities:** The most important diel variability in communities and relative
335 biomass/abundance was observed in the SSL (i.e. above 200m) (Fig. 3, 4, 5). The gelatinous MM
336 (mainly salps) dominated biomass at nighttime at M1 and M2 and abundance at M1. During the night
337 at M2, gelatinous groups and crustaceans were rather balanced in terms of relative abundance in the top
338 200 m layer. Crustaceans (mainly euphausiids at M1, M3 and M4 at night, Fig. 7) were lower in
339 biomass but more abundant than gelatinous organisms. Myctophids (mainly *E. antarctica*, Fig. 8) were
340 only present in this surface layer during nighttime. Between 200 and 500 m, gelatinous MM (mostly
341 salps), contributed the most to total MM biomass during nighttime and a mixture with other gelatinous
342 during daytime at M1 and M2, while siphonophores dominates the biomass in this layer at M3 and M4
343 (Fig. 6). Crustaceans (mainly euphausiids and hyperiids, Fig. 7) were also proportionally abundant
344 during both periods of the day (Fig. 5), while numerous at this depth only at M2 (Fig. 7). Fish mainly
345 occurred in this MSL during night-time (Fig. 8). Below 500 m (excluding the station M2), the biomass
346 volume was shared between the three main taxonomic groups, with a higher contribution of fish than in
347 the upper layers (Fig. 4, 5). This corresponded with higher myctophid abundance and also more
348 bathylagids and cyclothones (supplemental material 1). Similar (relative) biomass and abundance were
349 observed during night-time and daytime within this DSL. Gelatinous organisms were similar to the
350 MSL previously described with an increased proportion of jellyfish occurring during night-time (Fig.
351 6). Crustaceans presented similar biomass between night-time and daytime.

352

353 *-Inter-station variability-* Lower biomass were reported for M3 and M4 stations during the nighttime in
354 the (sub-)surface (shallower than 200 m). This main difference was mostly attributed to gelatinous
355 organisms. While salps were abundant at M1 and M2 stations, they represented a low percentage of the
356 gelatinous community at M3 and M4 (Table 3 and Fig. 6). The biomass at these latter stations were
357 consequently considerably lower with a higher contribution of the other taxa, particularly
358 siphonophores (occurring only deeper than 300m, including at M2) and to a lesser extent, ctenophores
359 and jellyfish.

360 Crustacean abundances between stations exhibited a different pattern. They were numerous at the M2
361 station with a large proportion of the hyperiid *T. gaudichaudii* (Table 4 and Fig. 7). At other stations,
362 euphausiids dominated the crustacean community, especially in surface waters during nighttime where
363 large quantities were collected (at stations M1 and M4).

364 Conversely to the crustacean pattern, the lowest abundances of fish, including the dominant
365 myctophids, were found at M2. Despite a low fish biomass at this station, a high diversity was found

366 and *E. antarctica* was the most abundant species at all depths. At other stations, *K. anderssoni* was the
367 dominant species, particularly in mid-depth and deeper waters during nighttime. However, *E.*
368 *antarctica* was the most common species found in surface waters during the nighttime and at depth
369 during the daytime.

370 Finally, the main contrast observed in acoustic densities were reported between M2 and the other
371 stations (Fig. 9). The more similar pattern in the trawl results is observed for the fish, that are less
372 abundant at M2.

373

374 *-Intra-station variability-* For stations visited twice (M4) or three times (M2 and M3), patterns of
375 vertical distributions were coherent despite some variability was observed. The variability is mostly
376 observed in terms of biomass and abundance at similar depths, while the composition of the MM
377 community was similar between visits. Acoustic profiles indicated some changes observed between
378 visits. Densities observed during daytime at M2 decreased between the first (highest daytime biomass,
379 Fig. 3) and the second visit. At M3 and M4, a global deepening of densities from MSL to DSL (highest
380 fish biomass reported during the 2nd visit of M3) as well as an increase in the surface layer occurred
381 between the first and the second visit, especially during nighttime.

382

383 **- Description of the carbon content in each taxonomic group**

384 Due to low carbon content, the contribution of gelatinous plankton to total carbon biomass was
385 important but decreased significantly in comparison with their contribution to wet biomass (Fig. 11). At
386 most of the stations (M1, M3 and M4), fish dominated carbon biomass in the DSL, especially for the
387 night trawls. In surface layers, crustaceans were usually the major contributors to carbon biomass,
388 except for a few stations where gelatinous organisms were dominant.

389

390 **- Respiratory carbon flux**

391 The abundance, biomass, and respiratory carbon flux from myctophids entering the mesopelagic zone
392 ranged from 0.001 to 0.163 ind m⁻², from 0.04 to 15.08 mg C m⁻² d⁻¹, and from 0 to 0.045 mg C m⁻² d⁻¹,
393 respectively. According to Fig. 12, the stations M1 and M4 that were located over the ocean basin,
394 exhibited the highest values of abundance, biomass, and carbon export, while M2 and M3 (over and
395 close to the plateau, respectively) resulted in the lowest values. Averaged Chl *a*, from 20 to 100 m
396 depth, ranged from 0.19 to 0.60 mg m⁻³ during the visits at which carbon flux was estimated (Fig. 12a-
397 b). As a result of the varying hydrographic conditions found at each visit, the distribution of migratory
398 scattering layers changed, and the depth range of trawling was adjusted to target these layers (e-h). The

399 highest values on abundance, biomass, and carbon export coincided with intermediate Chl *a* values in
400 M1 and M4, in migratory layers sampled between 50 and 170 m depth (trawls 11, 21, 31 in Fig. 12),
401 while the lowest with Chl *a* maxima at M2, in migratory layers sampled between 30 and 90 m (trawls
402 37, 39 in Fig. 12). Carbon flux was fundamentally driven by biomass, which was in turn driven by the
403 total number of individuals in the catch. This resulted from the overall similar size distributions
404 between trawls, with individuals mostly ranging from 10 to 70 mm standard length (see supplementary
405 material 2). Exceptionally, in trawls 6 and 20 at M2 station, the occurrence of a few individuals larger
406 than 100 mm increased the total biomass, but decreased carbon export as result of lower metabolic
407 rates of large fish (see equation 1).

408 **Discussion**

409 The waters surrounding the Kerguelen Islands encompassed variable communities of MM, with respect
410 to their biomasses, proportional contributions, and vertical patterns. Because vertical active fluxes are
411 generally driven by biomass and composition, this has important implications for the regional and
412 global biological pump (Ariza et al., 2015, Gorgues et al., 2019, Hernández-León et al., 2019). The
413 MM variability had been revealed in this study in response to the particular physical features and
414 biological characteristics of this dynamic area. While the combination of trawl and acoustic sampling
415 clearly benefited the description of the MM community, it is crucial to bear in mind the specificities of
416 each methodology (Ariza et al., 2016). Despite the possibility of contamination of deep hauls by upper
417 organisms due to the use of a non-closing trawl, we reduced this effect through fast launch and haul out
418 during trawl operations. Moreover, while numerous species were sampled we only focus on the most
419 abundant species. This precaution is particularly adapted in our study area where the dominant species
420 were limited and represent a very high proportion in terms of biomass-abundance, consequently
421 contributing significantly to the backscatter. In turn, acoustic measurements are based on the properties
422 of the dominant species in a volume containing many organisms, either in terms of relative backscatter
423 intensity dominated by the strongest reflector or due to the frequency-dependent response. It implies
424 that gas-bearing organisms such as fish with air-filled swimbladders or siphonophores dominated small
425 fluid-like organisms at 18kHz and 38kHz (Ariza et al., 2016, Behagle et al., 2017).

426

427 **1. Macrozooplankton-micronekton communities within the Kerguelen seascape and spatial** 428 **variability.**

429 Our results provide a comprehensive picture of the macrozooplankton-micronekton (MM) communities
430 following a longitudinal gradient across the Kerguelen plateau, and serves as a case study of an area of
431 the Southern Ocean where contrasted production regions occur. The set of four stations visited during
432 the survey represented different environments describing the various seascape around the Kerguelen
433 Islands. These environments differed in terms of bathymetry (downstream vs upstream location relative
434 to the plateau), level of biological production (Chl *a*) and northern vs southern location in relation to
435 the PF.

436 - **M1 was representative of the Kerguelen plume** downstream of the plateau. At this location close to
437 the PF, the primary production peaked three months earlier and was very low during the cruise. Salps
438 largely dominated the biomass, especially during night-time in the SSL and MSL. Euphausiids, mainly
439 *E. vallentini*, was abundant in surface layers during night-time. Significant abundance of the fish

440 species *K. anderssoni* and *E. antarctica* were found within the SSL to DSL, according to their diel
441 cycle (Duhamel et al. 2000). This area on the eastern flank of the Kerguelen plateau is a well-known
442 foraging area for top predators such as king penguins, macaroni penguins and fur seals, which
443 predominantly forage within the SSL on crustaceans and myctophids (Bost et al., 2002, Lea and
444 Dubroca 2003, Sato et al., 2004)

445 - **M2 was representative of the productive plateau area**, even if relatively low Chl *a* was estimated
446 during the sampling period, it was preceded by a strong bloom. Indeed, this area is characterized by a
447 reoccurring large phytoplankton bloom induced by naturally iron-fertilized waters from the plateau
448 (Blain et al., 2007). Trawl estimated MM biomass was high at this station with salps being the main
449 contributors. Crustaceans were numerous at M2, with a large proportion of *T. gaudichaudii*, as
450 previously reported (Carlotti et al., 2015), followed by *E. vallentini*. Fish densities were the lowest at
451 M2 compared to other stations, while their diversity was the highest. Sustained blooms as observed on
452 the plateau station favour a high secondary production rate and a general increase in herbivory in
453 zooplankton, as observed during the KEOPS2 survey (Carlotti et al., 2015).

454 - **M3 was the first HNLC upstream station north of the PF**; it was located close to the plateau and
455 corresponded to the previous KERFIX station (Jeandel et al. 1998). The lowest overall biomass was
456 reported at this station mainly due to low salp densities. However, the gelatinous group had a relatively
457 high diversity, with a contribution of siphonophores, jellyfish and ctenophores. Crustacean abundance
458 was low and dominated by euphausiids. As a consequence of the low contribution of other groups, fish
459 made a relatively high contribution to biomass at M3. Their densities were highly variable and they
460 were more diverse, with less *E. antarctica* and a higher proportion of bathylagids and *Cyclothone* sp.
461 The observed community corresponded to warmer waters north of the PF delimiting the northern extent
462 of the distribution area of the endemic Antarctic *E. antarctica* (Duhamel et al., 2014).

463 - **M4 was the second HNLC upstream station south of the PF**. This station was located further west
464 from the plateau. The gelatinous group dominated the total biomass, with siphonophores ranking first,
465 salps showing the lowest contribution, and jellyfish being significant in the deeper layers. Euphausiids
466 dominated crustaceans and their total densities within the SSL. Fish made a larger contribution at night
467 than during the day, and *K. anderssoni* and *E. antarctica* were equally important contributors. Within
468 the M3 and M4 areas, upstream of the plateau, the PF location is highly variable and undergoes a large
469 seasonal change (Pauthenet et al., 2018). These authors reported that the PF is located at its southern
470 position in March, i.e., during the survey period. As a consequence, the location of station M3 in
471 relation to the PF may have shifted in the previous months and resulted in different physical and
472 biogeochemical conditions. Moreover, the purported HNLC upstream M3/M4 stations presented

473 similar levels of Chl *a* than the downstream M1 station. The production at M3/M4 was abnormally
474 high when compared to the averaged Chl *a* (Christaki et al., this issue), potentially influencing the
475 densities of the MM populations.

476

477 **2. Diel cycles and intra-station variability as sources of time varying patterns**

478 Despite clear differences in vertical distribution of both acoustic densities and biomass-abundance
479 between daytime and nighttime, a consistent three-layers system occurred over the whole Kerguelen
480 area from upstream to downstream regions of the plateau. Here we describe and interpret the temporal
481 variability due to this diel cycle, together with the variability observed between visits at the same
482 stations

483 **- Diel vertical patterns of macrozooplankton-micronekton:**

484 While a higher total biomass was observed during nighttime, particularly in the surface layer, acoustic
485 densities were remarkably similar between daytime and nighttime.

486 - This acoustic peculiarity is especially noticeable in the SSL where various densities were reported at
487 the two frequencies. Here, very few gelatinous organisms and fish were collected and nearly-only
488 crustaceans were trawled during daytime. The combination of trawl avoidance from myctophids during
489 daylight and of their diurnal behaviour in the structuring could explain why biomass of these organisms
490 are undersampled in the surface layer (Kaartvedt et al., 2012). Indeed, fish schooling is a diurnal
491 behaviour leading to a patchy distribution during the day that vanishes at night (Saunders et al., 2013).
492 The peak in acoustic densities above 100 m during daytime is likely to correspond to a thin layer where
493 small schools of myctophids probably occurred. This is suggested by both previous acoustic
494 measurements carried out in the area east of the plateau corresponding to the station M1 (Behagle et al.,
495 2017), and the diving depth of king penguins that feed mostly on *K. anderssoni* during daytime
496 (Scheffer et al., 2016). Few fish species were caught at shallow depths in offshore Kerguelen waters
497 during the day, with the shallow acoustic densities being likely *K. anderssoni* (Duhamel et al., 2000).
498 The vertical distribution of this non-migratory species is based on age-segregation: juveniles are
499 intensively feeding in the warm and productive surface waters while adults were found deeper
500 (Lourenço et al., 2017).

501

502 - The diel cycle in the upper layer was the largest contrast we observed, with the invasion of gelatinous,
503 crustaceans and mesopelagic fish from mid- and deep layers to the epipelagic. The daily difference in
504 biomass and in the RGB echograms evidenced the migratory pattern of numerous species, including:

505 i) salps, which were found deeper than 200 m in the morning and performed a first migration to
506 subsurface at mid-day, before moving up to the surface layer at night (Nishikawa and Tsuda 2001,
507 Henscke et al., 2021).
508 ii) the main crustacean species, i.e. *E. vallentini* that performed DVM from subsurface-deep waters
509 (100 m to 600 m depth) during daytime to the surface layer during night-time (Mauchline and Fisher,
510 1969, Boden and Parker, 1986), and *T. gaudichaudii* that also displayed DVM through a more complex
511 pattern due to an ontogenetic component, with juveniles moving in the upper 100 m whereas adults
512 descended to depths below 200 m during daytime (Pakhomov and Froneman, 1999).
513 iii) the myctophid *E. antarctica* exhibits a typical DVM, occurring within the surface waters during the
514 night and descending below 300 m during daytime, with a size component (larger individuals found
515 deeper than 600 m at night, while small fish were located at 300-400 m during the day; Hulley and
516 Duhamel, 2011). Meanwhile, other important contributors are non- or slightly migratory species, such
517 as *K. anderssoni* (see above) and the siphonophore *R. plicata* that exhibits a quasi-permanent
518 distribution below 300 m with minor diel movements (as suggested in Pugh 1984).

519

520 - Multiple layers and patches and diverse DVM during the transition periods were observed on the
521 RGB echograms. This bi-frequency visualization is particularly insightful to understand the vertical
522 patterns of averaged acoustic profiles that appeared relatively similar during both day and night
523 periods. Here we attempt to interpret this three-layer system based on the combination of bi-frequency
524 responses and trawl sampling obtained during our survey and on the already known diel vertical
525 distribution:

526 - SSL: During daytime, this layer was dominated by juveniles of *K. anderssoni* and of *T.*
527 *gaudichaudii*, while it was invaded by numerous species at night from deeper waters, including salps,
528 *E. antarctica*, and *E. vallentini*. First preliminary results from the four frequency comparison (but
529 limited to the surface layer) indicated a more complex pattern with layers presenting multi-acoustic
530 responses indicative of multi-species structures.

531 - MDL: During daytime, salps distributed in the upper part (~200 m) of this layer at M1 in the
532 morning, before moving up at mid-day, as indicated by a strong response at 18kHz (Wiebe et al., 2010).
533 A mix of the main crustacean species (*E. vallentini* and adults *T. gaudichaudii* between 200 m and 300
534 m) was found at M2. The lower part was attributed to siphonophores collected below 300 m, combined
535 with crustaceans. During night-time, crustaceans mainly migrated to the SSL, while siphonophores
536 constituted a permanent layer below 300 m, slightly moving upward at night. At the M2 station, waters

537 just above the bottom were characterized by a permanent layer that was found deeper (~600 m) at the
538 other stations.

539 - DSL: During daytime, the permanent 38kHz-dominated layer centred at 600 m was probably
540 characterized by the main fish species in the area, i.e., large specimens of *E. antarctica*, adults of *K.*
541 *anderssoni*, and bathylagids and *Cyclothone* sp. together with siphonophores and euphausiids. During
542 the night, a part of this fish community, probably juveniles or the smallest individuals, move upward
543 together with euphausiids. However, a 600 m-depth layer remained permanently, with the same
544 combination of organisms that was acoustically dominated by fish. The higher 38kHz acoustic levels
545 compared to the 18kHz at the DSL could originate from this fish dominance, since larger non-migrant
546 *E. antarctica* individuals have a reduced gaseous swimbladder relative to the smaller individuals that
547 have a large air-filled swimbladder (Dornan et al. 2019). Other acoustic layers occurred deeper, at the
548 limit of the 38kHz vertical range, where just two trawls were carried out and reported a similar
549 community with more deep-sea species such as jellyfish.

550 - **Intra-station variability of vertical patterns:**

551 The vertical patterns in biomass and communities together with the diel cycles were coherent between
552 visits at the M2 station and at the two upstream M3/M4 stations. While M1 appeared to be a physical
553 dynamic area and the other stations showed a low horizontal transport (Henschke et al., 2021), the
554 trawl data indicate that the same MM populations were sampled at each station. The occasional
555 variability in biomass and abundance in the same layers could indeed be attributed either to the known
556 MM patchiness (i.e., spatial variability) or to the development of trophic interactions (i.e., temporal
557 variability).

558 Noticeable variability was observed between the first and following two visits to M2, with a decrease
559 in daytime acoustic density at 200 m and an overall larger biomass of crustaceans during the second
560 visit. An increase and deepening of densities from the MSL to DSL was observed at M3 during night-
561 time, which was confirmed by a higher biomass of all taxa, i.e. *K. anderssoni*, *E. vallentini* and
562 siphonophores.

563

564

565 **3. Variability in vertical distribution of carbon content and active flux associated with** 566 **macrozooplankton-micronekton.**

567 For consistency, we used an average of water carbon content computed for each of the groups, based on
568 available data from the literature. However, we acknowledge that variability can be observed between
569 species of the groups and between different estimates within the same species. Such variability can be

570 explained by the different geographic area where the same species occurred and the samples obtained at
571 different seasons, both potentially affecting the body composition of organisms (Schaafsma et al 2018).
572 Although gelatinous groups dominated the wet biomass in the majority of trawls, it is the energy
573 content that is important to sustain the development of higher trophic levels. For example, crustaceans
574 are higher quality food than gelatinous organisms, such as salps (Harmelin-Vivien et al 2019).
575 Considering C content allows a better estimate of the relative contribution of the different groups in
576 terms of their roles in the energy transfer along the food web. Mesopelagic fish represented the main
577 source of carbon stock in the DSL. They were shown to play an important role in active transfer of
578 carbon from the intermediate layers to deep waters (Irigoiien et al 2014). The extent of the active carbon
579 flux driven by fish depends on the species composition, with not all species performing DVM
580 (Romero-Romero et al 2019, Klevjer et al 2020). In our study, some of the highest fish C biomasses
581 were measured at the station M3, where relatively low abundances of crustacean were found in the
582 upper layer (including zooplankton, see Hunt et al this issue), potentially implying some top down
583 control. However, primary productivity in surface waters at this upstream station was low, which may
584 have contributed to the low crustacean biomass, and further, it is questionable whether such low
585 biomass of fish can impact crustacean abundance (Pepin et al 2013). Crustacean and gelatinous
586 organisms represented a large, although varying C stock at the 'productive' station M2, but they were
587 not associated with a high mesopelagic fish biomass, possibly due to depth limitation (ca 550 m depth
588 over the shelf).

589
590 Additionally, we only estimated the respiratory carbon flux mediated by migratory fish from the family
591 Myctophidae, a major component in the Southern Ocean food web (Pakhomov et al., 1996; Saunders et
592 al., 2019), which is known to play an important role in the active transport of carbon to the deep ocean
593 (Davison et al., 2013; Ariza et al., 2015; Belcher et al., 2019; Kwong et al., 2020). Interestingly here,
594 myctophids ranked as the fourth group contributing to migrant biomass, after gelatinous organisms and
595 crustaceans, mainly salps, euphausiids, and hyperiids (Fig. 3-8). Without discrediting the important role
596 of these groups in the Antarctic food webs (Perissinoto et al., 1998; Pakhomov et al., 2002), it should
597 be taken into account that our results on relative biomass among groups might be strongly affected by
598 the catchability and selectivity performance of our trawling net (Meillat, 2012, Béhagle et al., 2017).
599 Myctophids are fast swimmers and they are expected to efficiently avoid trawling nets (Kaarvedt et al.,
600 2012), especially when compared to quasi-drifting life forms like salps, or to smaller organisms such as
601 euphausiids or hyperiids (Skjoldal, et al. 2013). Trawl avoidance can make a difference, considering
602 that we used a net with a 65 m² mouth area. Hence, we presumed that myctophids were undersampled

603 and are an overwhelmingly important component of the DVM in the study region. This, along with the
604 extraordinary migration extent of organisms, often beyond 700-800 m depth when they are larger than
605 40 mm (Badcock and Merret, 1976), made pertinent the estimation of carbon flux on this group which
606 required further investigations.

607

608 Our carbon flux estimation relies on individual body mass and environmental temperature, using a
609 respiration rate predictive equation for myctophids, implemented by Belcher et al (2019). As discussed
610 by the authors of this work, species-specific metabolism variance is not accounted for by this predictive
611 equation and this should be added, along with the capture efficiency of the net, as factors potentially
612 influencing our results. Capture efficiency and metabolic models are a common source of uncertainty
613 to estimate carbon flux in micronekton, and this might explain why results generated over the last two
614 decades still differ by up to three orders of magnitude (see Table 6). Our respiratory carbon flux
615 estimations, ranging from 0.001 to 0.045 mg C m⁻² d⁻¹, are for instance one order or magnitude lower
616 than those obtained by Belcher et al. (2019) in the Atlantic sector of the Southern Ocean, using the
617 same predictive equation, and based on non-corrected catch data, as we did (see Table 6). This
618 demonstrates the urgent need to perform further inter-calibration experiments on micronekton samplers
619 and acoustics (Pakhomov et al., 2010, Kaartvedt et al., 2012), and to work towards obtaining more
620 accurate metabolic models for species involved in DVM (Becher et al., 2019, 2020). In the particular
621 case of this study, the mesopelagos net is known to strongly undersample large fish (Meillat, 2012,
622 Béhagle et al., 2017). Respiration is also expected to be underestimated in cold temperature
623 environments, because the predictive equation was partially built from respiration rates calculated for
624 temperate and tropical species (Belcher et al., 2020). Our carbon flux estimations might therefore be
625 underestimated to an unknown degree, but until these uncertainties are resolved, the results should be
626 interpreted with caution in absolute terms. Indeed, the most recent inter-comparison of carbon fluxes
627 between epi- and mesopelagic zones using a linear inverse ecosystem model suggested that estimates of
628 zooplankton active transport using conservative estimates of standard metabolism are grossly
629 underestimated (Kelly et al. 2020). Relative values among stations and visits were however revealing
630 about how environmental factors and population dynamics can affect carbon flux. For instance, Figure
631 12 illustrates how carbon flux is strongly driven by the total migrant biomass, but that this biomass will
632 be more efficiently converted into carbon dioxide when the size structure of the community is small.
633 This results from higher metabolic rates occurring in small fish (Equation 1). On the other hand, the
634 migration range in small myctophid fishes used to be shorter and shallower (Badcock and Merrett,
635 1976), and this should be taken into account when modelling fish-mediated carbon export. Overall, the

636 ocean-basin and slope-boundary stations M1 and M4, situated south off the PF, had greater migrant
637 biomass, larger species, and from twofold to threefold higher respiratory carbon fluxes. This highlights
638 the importance of patchiness when assessing carbon export, and demonstrate a strong bottom up
639 structuring on this mechanism.

640

641 **Conclusion**

642 We used a complementary collection of trawl and acoustic data to elucidate MM biodiversity and its
643 organisation in the different primary production regimes in the Kerguelen region. We identified a
644 variable three-layer system common to the zones over and around the Kerguelen plateau, a shallow
645 scattering layer (SSL, between 10 and 200 m), mid-depth scattering layers (MSL, between 200 and 500
646 m) and deep scattering layers (DSL, between 500 and 800 m). This integrated trawl–acoustic approach
647 is needed to collect the necessary information to understand the patterns of variability in mesopelagic
648 ecosystems, including diversity and vertical distribution, and their consequences in terms of trophic
649 interactions and biogeochemical fluxes. Next steps will be to use the full range of acoustic frequencies
650 (18 kHz to 200 kHz) to better resolve the complexity of the various groups, despite limited to the SSL.
651 The biophysical links also deserve investigations to describe the influence of physical features such as
652 the stratification of water masses, the PF and the plateau vs offshore areas. Finally, estimates of active
653 C fluxes should be made to other groups in addition to fish, to reach an assessment of the combined
654 active contribution of mid-trophic levels on the biological carbon pump.

655

656 **Acknowledgements**

657 We thank B. Quéguiner, the PI of the MOBYDICK project, for providing us the opportunity to
658 participate to this cruise, the chief scientist I. Obernosterer and the captain and crew of the R/V Marion
659 Dufresne for their enthusiasm and support aboard during the MOBYDICK–THEMISTO cruise
660 (<https://doi.org/10.17600/18000403>). This work was supported by the French oceanographic fleet
661 (“Flotte océanographique française”), the French ANR (“Agence Nationale de la Recherche”, AAPG
662 2017 program, MOBYDICK Project number : ANR-17-CE01-0013), and the French Research program
663 of INSU-CNRS LEFE/CYBER (“Les enveloppes fluides et l’environnement” –“Cycles
664 biogéochimiques, environnement et ressources”). This research was partially supported by the Cnes
665 OSTST Tosca project LAECOS, BEST program IUCN-European Commission (SECTOR grant
666 agreement No 2279) and H2020 (MESOPP grant agreement No 692173) held by CC. The authors
667 acknowledged Aviso, ACRI-ST and the European Copernicus Marine Environment Monitoring Service
668 for the production and the delivery of environmental data.

669 **References**

- 670 Anderson, T.R., Martin, A.P., Lampitt, R.S., Trueman, C.N., Henson, S.A., Mayor, D.J., 2018.
671 Quantifying carbon fluxes from primary production to mesopelagic fish using a simple food web
672 model. *ICES J. Mar. Sci.* 76, 690–701. <https://doi.org/10.1093/icesjms/fsx234>
- 673 Annasawmy, P., Ternon, J.-F., Cotel, P., Cherel, Y., Romanov, E.V., Roudaut, G., Lebourges Dhaussy,
674 A., Ménard, F., Marsac, F. 2019. Micronekton distributions and assemblages at two shallow seamounts
675 of the south-western Indian Ocean : insights from acoustics and mesopelagic trawl data. *Prog.*
676 *Oceanogr.* 178, art. 102161.
- 677 Ariza, A., Garijo, J.C., Landeira, J.M., Bordes, F., Hernández-León, S., 2015. Migrant biomass and
678 respiratory carbon flux by zooplankton and micronekton in the subtropical northeast Atlantic Ocean
679 (Canary Islands). *Prog. Oceanogr.* 134, 330–342.
- 680 Ariza, A., Landeira, J. M., Escánez, A., Wienerroither, R., Aguilarde Soto, N., Røstad, A., Kaartvedt,
681 S., and Hernández-León, S. 2016. Vertical distribution, composition and migratory patterns of acoustic
682 scattering layers in the Canary Islands, *J. Mar. Syst.*, 157, 82–91.
683 <https://doi.org/10.1016/j.jmarsys.2016.01.004,2016>.
- 684 Badcock, J., Merrett, N.R., 1976. Midwater fishes in the eastern North Atlantic—I. Vertical distribution
685 and associated biology in 30N, 23W, with developmental notes on certain myctophids. *Prog. Oceanogr.*
686 7, 3–58.
- 687 Béhagle, N., Cotté, C., Lebourges-Dhaussy, A., Roudaut, G., Duhamel, G., Brehmer, P., Josse, E.,
688 Cherel, Y., 2017. Acoustic distribution of discriminated micronektonic organisms from a bi-frequency
689 processing: The case study of eastern Kerguelen oceanic waters. *Prog. Oceanogr.* 156, 276–289.
- 690 Belcher, A., Cook, K., Bondyale-Juez, D., Stowasser, G., Fielding, S., Saunders, R.A., Mayor, D.J.,
691 Tarling, G.A., 2020. Respiration of mesopelagic fish: a comparison of respiratory electron transport
692 system (ETS) measurements and allometrically calculated rates in the Southern Ocean and Benguela
693 Current. *ICES J. Mar. Sci.* fsaa031.
- 694 Bianchi, D., Stock, C., Galbraith, E. D., Sarmiento, J. L., 2013. Diel vertical migration: Ecological
695 controls and impacts on the biological pump in a one-dimensional ocean model. *Global Biogeochem.*
696 *Cycles* 27, 478–491. <https://doi:10.1002/gbc.20031>
- 697 Blain, S., et al., 2007. Effect of natural iron fertilization on carbon sequestration in the Southern Ocean.
698 *Nature* 446, 1070–1074. <https://doi:10.1038/nature05700>.
- 699 Bocher, P., Cherel, Y., Labat, J.P., Mayzaud, P., Razouls, S., Jouventin, P., 2001. Amphipod-based food
700 web: *Themisto gaudichaudii* caught in nets and by seabirds in Kerguelen waters, southern Indian
701 Ocean. *Mar. Ecol. Prog. Ser.* 223, 261–276.
- 702 Boden, B. P., Parker, L. D., 1986. The plankton of the Prince Edward Islands. *Polar Biol.* 5, 81–93.
- 703 Bost, C., Zorn, T., Le Maho, Y., Duhamel, G., 2002. Feeding of diving predators and diel vertical
704 migration of prey: King penguin's diet versus trawl sampling at Kerguelen Islands *Mar. Ecol. Prog. Ser.*
705 227, 51–61.

- 706 Brett, J.R., 1979. Factors affecting fish growth, in Fish Physiology Volume 8 (eds W.S. Hoar, D.J.
707 Randall and J.R. Brett), Academic Press, New York, pp. 599–675.
- 708 Carlotti, F., Jouandet, M.-P., Nowaczyk, A., Harmelin-Vivien, M., Lefèvre, D., Richard, P., Zhu, Y.,
709 Zhou, M., 2015) Mesozooplankton structure and functioning during the onset of the Kerguelen
710 phytoplankton bloom during the KEOPS2 survey, Biogeosciences 12, 4543–4563,
711 <https://doi.org/10.5194/bg-12-4543-2015>.
- 712 Cherel, Y., Bocher, P., de Broyer, C., Hobson, K.A., 2002. Food and feeding ecology of the sympatric
713 thin-billed *Pachyptila belcheri* and Antarctic *P. desolata* prions at Iles Kerguelen, Southern Indian
714 Ocean. Mar. Ecol. Prog. Ser. 228, 263–281.
- 715 Cherel, Y., Ducatez, S., Fontaine, C., Richard, P., Guinet, C., 2008. Stable isotopes reveal the trophic
716 position and mesopelagic fish diet of female southern elephant seals breeding on the Kerguelen Islands.
717 Mar. Ecol. Prog. Ser. 370, 239–247.
- 718 Christaki, U., Skouropoliakou, I.-D., Delegrange, A., Irion, S., Courcot, L., Jardillier, L., Sassenhagen, I.
719 Microzooplankton diversity and role in carbon cycle in contrasting Southern Ocean productivity
720 regimes. this issue
- 721 de Baar, H.J.W., de Jong, J.T.M., Bakker, D.C.E., Löscher, B.M., Veth, C., Bathmann, U., Smetacek,
722 V., 1995. Importance of iron for phytoplankton spring blooms and CO₂ drawdown in the Southern
723 Ocean. Nature 373, 412–415.
- 724 De Robertis, A., Higginbottom, I., 2007. A post-processing technique to estimate the signal-to-noise
725 ratio and remove echosounder background noise. ICES J. Mar. Sci. 64, 1282–1291.
- 726 d'Ovidio, F., Della Penna, A., Trull, T. W., Nencioli, F., Pujol, M.-I., Rio, M.-H., Park, Y.-H., Cotté, C.,
727 Zhou, M., Blain, S., 2015. The biogeochemical structuring role of horizontal stirring: Lagrangian
728 perspectives on iron delivery downstream of the Kerguelen Plateau. Biogeosciences 12, 5567–5581.
729 <https://doi.org/10.5194/bg-12-5567-2015>
- 730 Davison, P.C., Checkley, D.M., Koslow, J.A., Barlow, J., 2013. Carbon export mediated by
731 mesopelagic fishes in the northeast Pacific Ocean. Prog. Oceanogr. 116, 14–30.
- 732 Demer, D.A., Berger, L., Bernasconi, M., Bethke, E., Boswell, K., Chu, D., Domokos, R., et al.
733 2015. Calibration of acoustic instruments. ICES Cooperative Research Report No. 326. 133 pp.
734 <https://doi.org/10.17895/ices.pub.5494>
- 735 Dornan, T., Fielding, S., Saunders, R.A., Genner, M.J., 2019. Swimbladder morphology masks
736 Southern Ocean mesopelagic fish biomass. Proc. R. Soc. B. 286, 20190353.
737 <http://doi.org/10.1098/rspb.2019.0353>
- 738 Duhamel, G., Koubbi, P., Ravier, C., 2000. Day and night mesopelagic fish assemblages off the
739 Kerguelen Islands (Southern Ocean). Polar Biol. 23, 106–112.
- 740 Duhamel, G., Hulley, P.A., Causse, R., Koubbi, P., Vacchi, M., Pruvost, P., Vignetta, S., Irisson,
741 J.O., Mormède, S., Belchier, M., Dettai, A., Detrich, H.W., Gutt, J., Jones, C.D., Kock, K.H., Lopez
742 Abellan, L.J., Van de Putte, A.P., 2014. Biogeographic patterns of fish. Biogeographic Atlas of the
743 Southern Ocean, 7, 328–362.

- 744 Gorgues, T., Aumont, O., Memery, L., 2019. Simulated changes in the particulate carbon export
745 efficiency due to diel vertical migration of zooplankton in the North Atlantic. *Geophys. Res. Lett.* 46,
746 5387–5395. <https://doi.org/10.1029/2018GL08174>
- 747 Guinet, C., Cherel, Y., Ridoux, V., Jouventin, P., 1996. Consumption of marine resources by seabirds
748 and seals in Crozet and Kerguelen waters: changes in relation to consumer biomass 1962-85. *Antarct.*
749 *Sci.* 8, 23-30.
- 750 Harmelin-Vivien, M., Bănar, D., Dromard, C. R., Ourgaud, M., Carlotti, F., 2019. Biochemical
751 composition and energy content of size-fractionated zooplankton east of the Kerguelen Islands. *Polar*
752 *Biol.* 42, 603-617. doi:10.1007/s00300-019-02458-8
- 753 Harris, R.P., Wiebe, P., Lenz, J., Skjoldal, H.R., Huntley, M., 2000. *Zooplankton Methodology*
754 *Manual*, Academic, London, U.K.
- 755 Haury, L.R., McGowan, J.A., Wiebe, P.H., 1978. Patterns and processes in the time-space scales of
756 plankton distributions. In: Steele JH, editors. *Spatial patterns in plankton communities*. Plenum Press,
757 New York. 277–327.
- 758 Henschke, N., Blain, S., Cherel, Y., Cotté, C., Espinasse, B., Hunt, B.P.V., Pakhomov, E.A., 2021.
759 Population demographics and growth rate of *Salpa thompsoni* on the Kerguelen Plateau. *J. Mar. Syst.*
760 214, 103489.
- 761 Hernández-León, S., Olivar, M. P., Luz, M., De Puellas, F., Bode, A., Castellón, A., López-pérez, C. et
762 al., 2019. Zooplankton and micronekton active flux across the tropical and subtropical Atlantic Ocean.
763 *Front. Mar. Sci.* 6, 1–20.
- 764 Hernández-León, S., Koppelman, R., Fraile-Nuez, E. et al., 2020. Large deep-sea zooplankton
765 biomass mirrors primary production in the global ocean. *Nat. Commun.* 11, 6048.
766 <https://doi.org/10.1038/s41467-020-19875-7>
- 767 Hindell, M.A., Lea, M.-A., Bost, C.A., Charrassin, J.-B., Gales, N., Goldsworthy, S.D., Page, B.,
768 Robertson, G., Wienecke, B., O’Toole, M., Guinet, C., 2011. Foraging habitats of top predators, and
769 areas of ecological significance, on the Kerguelen Plateau. In: Duhamel, G., Welsford, D.C. (Eds.), *The*
770 *Kerguelen Plateau: Marine Ecosystem and Fisheries*. Société Française d’Ichtyologie, Paris, 203–215.
- 771 Hulley, P.A., Duhamel, G., 2011. Aspects of lanternfish distribution in the Kerguelen Plateau
772 region. In: G. Duhamel and D.C. Welsford (Eds). *The Kerguelen Plateau: marine ecosystems and*
773 *fisheries*. Société Française d’Ichthyologie, Paris, 183–195
- 774 Hunt, B.P.V., Pakhomov, E.A., Williams, R., 2011. Comparative analysis of the 1980s and 2004
775 macrozooplankton composition and distribution in the vicinity of Kerguelen and Heard Islands:
776 seasonal cycles and oceanographic forcing of long-term change. In: Duhamel, G., Welsford, D. (Eds.),
777 *The Kerguelen Plateau: Marine Ecosystem and Fisheries*. Société Française d’Ichtyologie, Paris, 79–
778 92.
- 779 Hunt, B.P.V., Espinasse, B., Henschke, N., Cherel, Y., Cotté, C., Delegrange, A., Pakhomov, E.A.,
780 Planchon F. Trophic pathways and transfer efficiency from phytoplankton to micronekton under
781 contrasting productivity regimes in the Kerguelen Islands region, Southern Ocean. This issue

- 782 Huntley, M.E., Sykes, P.F., Marin, V., 1989. Biometry and trophodynamics of *Salpa thompsoni* Foxton
783 (Tunicata, Thaliacea) near the Antarctic Peninsula in austral summer, 1983–1984. *Polar Biol.* 10, 59–
784 70.
- 785 Irigoien, X., Klevjer, T. A., Røstad, A., Martinez, U., Boyra, G., Acuña, J. L., et al., 2014. Large
786 mesopelagic fishes biomass and trophic efficiency in the open ocean. *Nat. Commun.* 5, 3271.
787 doi:10.1038/ncomms4271
- 788 Jeandel, C., Ruiz-Pino, D., Gjata, E., Poisson, A., Brunet, C., Charriaud, E., Dehairs, F., Delille, D.,
789 Fiala, M., Fravallo, C., Miquel, Jc., Park, Hy., Pondaven, P., Queguiner, B., Razouls, S., Shauer, B.,
790 Treguer, P., 1998. KERFIX, a time-series station in the Southern Ocean: a presentation. *J. Mar. Syst.*
791 17, 555-569. [https://doi.org/10.1016/S0924-7963\(98\)00064-5](https://doi.org/10.1016/S0924-7963(98)00064-5)
- 792 Kaartvedt, S., Staby, A., Aksnes, D.L., 2012. Efficient trawl avoidance by mesopelagic fishes causes
793 large underestimation of their biomass. *Mar. Ecol. Prog. Ser.* 456,1-6.
794 <https://doi.org/10.3354/meps09785>
- 795 Kelly, T.B., Davison, P.C., Goericke, R., Landry, M.R., Ohman, M.D., Stukel, M.R., 2019. The
796 importance of mesozooplankton diel vertical migration for sustaining a mesopelagic food web. *Front.*
797 *Mar. Sci.* 6,508. doi: 10.3389/fmars.2019.00508
- 798 Klevjer, T.A., Melle, W., Knutsen, T., Aksnes, D.L., 2020. Vertical distribution and migration of
799 mesopelagic scatterers in four north Atlantic basins. *Deep Sea Res. Part II.* 104811.
800 <https://doi.org/10.1016/j.dsr2.2020.104811>
- 801 Koubbi, P., Hulley, P.A., Raymond B., Penot, F., Gasparini, S., Labat, J.-P., Pruvost P., Mormède, S.,
802 Irisson, J.O., Duhamel, G., Mayzaud, P., 2011. Estimating the biodiversity of the sub-Antarctic
803 Indian part for ecoregionalisation: Part I. Pelagic realm of CCAMLR areas 58.5.1 and 58.6.
804 CCAMLR. WS-MPA-11/11, 1-39.
- 805 Kwong, L.E., Henschke, N., Pakhomov, E.A., Everett, J.D., Suthers, I.M., 2020. Mesozooplankton and
806 Micronekton Active Carbon Transport in Contrasting Eddies. *Front. Mar. Sci.* 6, 825. doi:
807 10.3389/fmars.2019.00825
- 808 Le Moigne, F.A.C., et al., 2016. What causes the inverse relationship between primary production and
809 export efficiency in the Southern Ocean? *Geophys. Res. Lett.* 43, 4457–4466.
810 doi:10.1002/2016GL068480
- 811 Larson, R.J., 1986. Water content, organic content and carbon and nitrogen composition of medusae
812 from the northeast Pacific. *J. Exp. Mar. Biol. Ecol.* 99, 107-120.
- 813 Lea, M.A., Cherel, Y., Guinet, C., Nichols, P.D., 2002. Antarctic fur seals foraging in the Polar Frontal
814 Zone: inter-annual shifts in diet as shown from fecal and fatty acid analyses. *Mar. Ecol. Prog. Ser.* 245,
815 281-297. [Erratum in *Mar Ecol Prog Ser* 253:310, 2003]
- 816 Lehodey, P., Conchon, A., Senina, I., Domokos, R., Calmettes, B., Jouanno, J., Hernández, O., Kloser,
817 R., 2014. Optimization of a micronekton model with acoustic data. *ICES J. Mar. Sci.* 72, 1399–1412.

- 818 Lourenço S., Saunders R.A., Collins M., Shreeve R., Assis C.A., Belchier M., Watkins J.L., Xavier
819 J.C., 2017. Life cycle, distribution and trophodynamics of the lanternfish *Krefftichthys anderssoni*
820 (Lönnberg, 1905) in the Scotia Sea. *Polar Biol.* 40, 1229-1245.
- 821 MacLennan, D.N., Fernandes, P., Dalen, J., 2002. A consistent approach to definitions and symbols in
822 fisheries acoustics. *ICES J. Mar. Sci.* 59, 365–369.
- 823 Maiti, K., Charette, M.A., Buesseler, K.O., Kahru, M., 2013. An inverse relationship between
824 production and export efficiency in the Southern Ocean. *Geophys. Res. Lett.* 40, 1557–1561.
825 [https://doi:10.1002/grl.50219](https://doi.org/10.1002/grl.50219)
- 826 Martin, A., Boyd, P., Buesseler, K., et al., 2020. The oceans' twilight zone must be studied now, before
827 it is too late. *Nature.* 580, 26-28. [https://doi:10.1038/d41586-020-00915-7](https://doi.org/10.1038/d41586-020-00915-7)
- 828 Mauchline, J., Fisher, L.R., 1969. The biology of euphausiids. *Adv. Mar. Biol.* 7, 1–454.
- 829 Meillat, M., 2012. Essais du chalut mésopélagos pour le programme MYCTO 3D - MAP de l'IRD, à
830 bord du Marion Dufresne (du 10 au 21 août 2012). Rapport de mission, Ifremer.
- 831 Mongin, M., Molina, E., Trull, T.W., 2008. Seasonality and scale of the Kerguelen plateau
832 phytoplankton bloom: a remote sensing and modeling analysis of the influence of natural iron
833 fertilization in the Southern Ocean. *Deep-Sea Res. Part II.* 55, 880–892.
834 <http://dx.doi.org/10.1016/j.dsr2.2007.12.039>.
- 835 Nishikawa, J., Tsuda, A., 2001. Diel vertical migration of the tunicate *Salpa thompsoni* in the Southern
836 Ocean during summer. *Polar Biol.* 24, 299-302
- 837 Pakhomov, E.A., Perissinotto, R., McQuaid, C.D., 1994. Comparative structure of the
838 macrozooplankton/micronekton communities of the Subtropical and Antarctic Polar Fronts. *Mar. Ecol.*
839 *Prog. Ser.* 111, 155–169.
- 840 Pakhomov, E., Perissinotto, R., McQuaid, C., 1996. Prey composition and daily rations of myctophid
841 fishes in the Southern Ocean. *Mar. Ecol. Prog. Ser.* 134, 1–14.
- 842 Pakhomov, E.A., Froneman, P.W., 1999. Macroplankton/micronekton dynamics in the vicinity of the
843 Prince Edward Islands (Southern Ocean). *Mar. Biol.* 134, 501–515.
- 844 Pakhomov, E.A., Yamamura, O., Brodeur, R.D., Domokos, R., Owen, K.R., Pakhomova, L.G.,
845 Polovina, J., Seki, M., Sunstov, A.V., 2010. Report of the advisory panel on micronekton sampling
846 inter-calibration experiment. *PICES Scientific Report* 38, 108.
- 847 Pauthenet, E., et al., 2018. Seasonal meandering of the polar front upstream of the kerguelen plateau.
848 *Geophys. Res. Lett.* 45, 9774–9781. doi:10.1029/2018GL079614
- 849 Pepin, P., 2013. Distribution and feeding of *Bentosema glaciale* in the western Labrador Sea: Fish–
850 zooplankton interaction and the consequence to calanoid copepod populations. *Deep Sea Res. Part I.*
851 75, 119-134. doi:<http://dx.doi.org/10.1016/j.dsr.2013.01.012>
- 852 Perrot, Y., Brehmer, P., Habasque, J., Roudaut, G., Behagle, N., Sarre, A., Lebourges-Dhaussy, A.,
853 2018. Matecho: An Open-Source Tool for Processing Fisheries Acoustics Data. *Acoust. Aust.* 46, 241–
854 248.

- 855 Pugh, P.R., 1984. The diel migrations and distributions within a mesopelagic community in the
856 Northeast Atlantic. 7. Siphonophores. *Prog. Oceanogr.* 13: 461–489.
- 857 Quéguiner, B., Blain, S., Trull, T., 2011. High primary production and vertical export of carbon over the
858 Kerguelen Plateau as a consequence of natural iron fertilization in a high-nutrient, low-chlorophyll
859 environment. In: Duhamel, G., Welsford, D. (Eds.), *The Kerguelen Plateau: Marine Ecosystem and*
860 *Fisheries*. Société Française d’Ichtyologie, Paris, 169-174.
- 861 Ratnarajah, L., Nicol, S., Bowie, A.R., 2018. Pelagic Iron Recycling in the Southern Ocean: Exploring
862 the Contribution of Marine Animals. *Front. Mar. Sci.* 5, 109. doi: 10.3389/fmars.2018.00109
- 863 Romero-Romero, S., Choy, C. A., Hannides, C. C. S., Popp, B. N., Drazen, J. C., 2019. Differences in
864 the trophic ecology of micronekton driven by diel vertical migration. *Limnol. Oceanogr.* 64, 1473-
865 1483. doi:10.1002/lno.11128
- 866 Ryan, T.E., Downie, R.A., Kloser, R.J., Keith, G., 2015. Reducing bias due to noise and attenua-
867 tion in open-ocean echo integration data. *ICES J. Mar. Sci.*, 72, 2482–2493.
- 868 Sato, K., Charrassin, J., Bost, C., Naito, Y., 2004. Why do macaroni penguins choose shallow body
869 angles that result in longer descent and ascent durations? *J. Exp. Biol.* 207, 4057–4065.
- 870 Saunders, R.A., Fielding, S., Thorpe, S.E., Tarling, G.A., 2013. School characteristics of mesopelagic
871 fish at South Georgia. *Deep Sea Res. Part I.* 81, 62-77. <https://doi.org/10.1016/j.dsr.2013.07.007>
- 872 Saunders, R.A., Hill, S.L., Tarling, G.A., Murphy, E.J., 2019. Myctophid Fish (Family Myctophidae)
873 Are Central Consumers in the Food Web of the Scotia Sea (Southern Ocean). *Front. Mar. Sci.* 6, 530.
- 874 Schaafsma, F.L., Cherel, Y., Flores, H. et al., 2018. Review: the energetic value of zooplankton and
875 nekton species of the Southern Ocean. *Mar. Biol.* 165, 129. <https://doi.org/10.1007/s00227-018-3386-z>
- 876 Scheffer, A., Trathan, P.N., Edmonston, J.G., Bost, C.-A., 2016. Combined influence of meso-scale
877 circulation and bathymetry on the foraging behaviour of a diving predator, the king penguin
878 (*Aptenodytes patagonicus*). *Prog. Oceanogr.* 141, 1–16.
- 879 Skjoldal, H.R., Wiebe, P.H., Postel, L., Knutsen, T., Kaartvedt, S., Sameoto, D., 2013. Intercomparison
880 of zooplankton (net) sampling systems: Results from the ICES/GLOBEC sea-going workshop. *Prog.*
881 *Oceanogr.* 108, 1–42.
- 882 Trenkel, V., Berger, L., Bourguignon, S., Doray, M., Fablet, R., Massé, J., Mazauric, V., Poncelet, C.,
883 Quemener, G., Scalabrin, C., et al., 2009. Overview of recent progress in fisheries acoustics made by
884 Ifremer with examples from the Bay of Biscay. *Aquat. Living Ressour.* 22, 433–445.
- 885 Wiebe, P.H., Chu, D., Kaartvedt, S., Hundt, A., Melle, W., Ona, E., Batta-Lona, P., 2010. The acoustic
886 properties of *Salpa thompsoni*. *ICES J. Mar. Sci.* 67, 583–593.

887 Table 1. EK80 echosounder settings.

888

Frequency (kHz)	Max. acquisition range (m)	Power (W)	Pulse length (μ s)
18	1000	2000	1024
38	800	1000	2048

889

Station	Visit	Date	Day/Night	Latitude/Longitude	Max depth (m)	Trawl ID	
M1	1st	08/03/18	Night	49°50 S / 74°54 E	51	21	
		08/03/18	Night	49°50 S / 74°54 E	290	22	
		08/03/18	Night	49°50 S / 74°54 E	617	23	
		09/03/18	Day	49°50 S / 74°54 E	400	24	
		09/03/18	Day	49°50 S / 74°54 E	50	25	
		09/03/18	Day	49°50 S / 74°54 E	632	26	
M2	1st	26/02/18	Day	50°36 S / 72°S	318	1	
		26/02/18	Day	50°30 S / 72°01 E	210	2	
		26/02/18	Day	50°27 S / 72° E	350	3	
		27/02/18	Night	50°35 S / 71°55 E	346	4	
		27/02/18	Night	50°35 S / 71°52 E	55	5	
		27/02/18	Night	50°34 S / 71°50 E	158	6	
	2nd	07/03/18	Day	50°39 S / 71°57 E	170	15	
		07/03/18	Day	50°39 S / 71°57 E	70	16	
		07/03/18	Day	50°39 S / 71°57 E	350	17	
		07/03/18	Night	50°40 S / 71°59 E	317	18	
		07/03/18	Night	50°40 S / 71°59 E	50	19	
		07/03/18	Night	50°40 S / 71°59 E	175	20	
	3rd	16/03/18	Night	50°36 S / 71°59 E	65	37	
		16/03/18	Night	50°36 S / 71°59 E	377	38	
16/03/18		Night	50°36 S / 71°59 E	30	39		
17/03/18		Day	50°36 S / 71°59 E	105	40		
17/03/18		Day	50°36 S / 71°59 E	340	41		
17/03/18		Day	50°36 S / 71°59 E	190	42		
M3	1st	04/03/18	Day	50°45 S / 68°03 E	55	13	
		04/03/18	Day	50°47 S / 68°01 E	460	14	
	2nd	15/03/18	Day	50°41 S / 68°03 E	683	33	
		15/03/18	Night	50°41 S / 68°03 E	610	34	
		15/03/18	Night	50°41 S / 68°03 E	90	35	
		15/03/18	Night	50°36 S / 67°58 E	415	36	
		3rd	18/03/18	Day	50°39 S / 67°45 E	814	43

	18/03/18	Day	50°39 S / 67°45 E	600	44
	18/03/18	Day	50°39 S / 67°45 E	65	45
	19/03/18	Night	50°39 S / 67°45 E	802	46
	19/03/18	Night	50°39 S / 67°45 E	650	47
	19/03/18	Night	50°39 S / 67°45 E	73	48
	01/03/18	Day	52°36 S / 67°11 E	93	7
	01/03/18	Day	52°35 S / 67°08 E	575	8
	01/03/18	Day	52°33 S / 67°00 E	425	9
1st	02/03/18	Night	52°36 S / 67°11 E	400	10
	02/03/18	Night	52°39 S / 67°07 E	96	11
	02/03/18	Night	52°42 S / 67°05 E	575	12
M4	14/03/18	Day	52°37 S / 67°09 E	85	27
	14/03/18	Day	52°37 S / 67°09 E	610	28
	14/03/18	Day	52°37 S / 67°09 E	410	29
2nd	14/03/18	Night	52°35 S / 67°11 E	600	30
	14/03/18	Night	52°35 S / 67°11 E	80	31
	14/03/18	Night	52°35 S / 67°11 E	400	32

893 Table 3. Proportion and occurrence of gelatinous species caught during trawl operations. Main
 894 contributions are in bold.

895

896

FAMILY	Species	% occurrence	% all stations	% M1	% M2	% M3	% M4
CHAETOGNATHS	<i>Sagitta gazellae</i>	93.62	0.77	0.43	0.62	3.56	1.34
CTENOPHORES	<i>Beroe cucumis</i>	31.91	0.89	0.75	0.21	2.33	2.95
	<i>Bolinopsis</i> sp.	29.79	0.74	0.24	0.09	11.98	0.09
	<i>Leucothea</i> sp.	2.13	0.01	0.00	0.00	0.17	0.00
MEDUSAE	<i>Atolla wyvillei</i>	17.02	1.53	0.62	0.00	14.36	4.42
	<i>Calyropsis borchgrevinki</i>	51.06	0.35	0.28	0.14	1.66	0.71
	<i>Calyropsis</i> sp. 2	6.38	0.02	0.00	0.00	0.31	0.00
	<i>Halicreas minimum</i>	2.13	0.00	0.00	0.00	0.05	0.00
	<i>Haliscera conica</i>	4.26	0.02	0.00	0.00	0.35	0.00
	Medusa unknown B	4.26	0.03	0.00	0.00	0.51	0.00
	<i>Periphylla periphylla</i>	29.79	1.02	0.05	0.19	5.92	5.00
	<i>Rhopalonema</i> sp.	2.13	0.01	0.00	0.00	0.00	0.05
	Scyphomedusae	2.13	0.05	0.00	0.00	0.00	0.40
	<i>Solmissus</i> sp. (<i>Medusa unknown A</i>)	36.17	0.37	0.27	0.00	1.38	1.47
	<i>Stygiomedusa gigantea</i>	0.00	0.00	0.00	0.00	0.00	0.00
NEMERTEANS	<i>Pelagonemertes rollestoni</i>	8.51	0.01	0.00	0.00	0.20	0.00
POLYCHAETES	<i>Tomopteris carpenteri</i>	17.02	0.01	0.01	0.02	0.03	0.00
SALPS	<i>Salpa thompsoni</i>	85.11	73.63	89.74	86.88	10.63	2.75
SIPHONOPHORES	<i>Diphyes</i> sp.	4.26	0.00	0.00	0.00	0.01	0.00
	<i>Rosacea plicata</i>	55.32	20.59	7.60	11.85	46.55	80.83

897

898 Table 4. Proportion and occurrence of crustaceans species caught during trawl operations. Main
 899 contributions are in bold.
 900

FAMILY	Species	% occurrence	% all stations	% M1	% M2	% M3	% M4
EUPHAUSIIDS	<i>Euphausia longirostris</i>	10.64	0.30	1.85	0.00	0.00	0.00
	<i>Euphausia triacantha</i>	82.98	11.28	15.71	7.20	20.03	9.99
	<i>Euphausia vallentini</i>	87.23	43.12	43.28	28.16	41.55	74.39
	<i>Thysanoessa macrura/vicina</i>	51.06	2.78	4.99	2.67	0.06	3.30
GAMMARID AMPHIPODS	<i>Cyphocaris richardi</i>	31.91	0.12	0.01	0.00	0.22	0.39
	<i>Danaela mimonectes</i>	10.64	0.01	0.00	0.00	0.01	0.02
	<i>Eurythenes obesus</i>	6.38	0.00	0.01	0.00	0.01	0.00
	<i>Eusiroides stenopleura</i>	19.15	0.03	0.02	0.00	0.10	0.07
	<i>Parandania boeckii</i>	40.43	0.89	1.55	0.08	2.22	1.11
HYPERIID AMPHIPODS	<i>Cylopus magellanicus</i>	80.85	0.87	2.27	0.89	0.25	0.24
	<i>Hyperia spinifera</i>	12.77	0.01	0.01	0.01	0.01	0.00
	<i>Hyperia macrocephala</i>	6.38	0.00	0.00	0.01	0.00	0.00
	<i>Hyperiella antarctica</i>	21.28	0.01	0.01	0.01	0.03	0.01
	<i>Hyperoche luetkenides</i>	44.68	0.07	0.11	0.09	0.03	0.02
	<i>Pegohyperia princeps</i>	2.13	0.00	0.00	0.00	0.00	0.00
	Physosomata sp. 1	6.38	0.00	0.00	0.00	0.02	0.00
	Physosomata sp. 2	4.26	0.00	0.01	0.00	0.00	0.00
	<i>Primno macropa</i>	87.23	1.65	2.07	1.52	3.44	0.44
	Scinidae sp.	0.00	0.00	0.00	0.00	0.00	0.00
	<i>Themisto gaudichaudii</i>	100.00	37.77	25.49	59.06	29.42	9.68
	<i>Vibilia antarctica</i>	72.34	0.59	2.44	0.25	0.40	0.05
MYSIDS	<i>Neognathophausia gigas</i>	8.51	0.01	0.00	0.00	0.04	0.00
	Mysida sp.	17.02	0.25	0.00	0.05	1.44	0.00
	Mysida sp. (red)	4.26	0.04	0.00	0.00	0.27	0.00
NATANTIA	<i>Acanthephyra pelagica</i>	4.26	0.00	0.00	0.00	0.01	0.00
	<i>Campylonotus</i> sp. (red)	21.28	0.01	0.02	0.00	0.03	0.00
	<i>Pasiphaea scotiae</i>	25.53	0.04	0.03	0.00	0.08	0.09
	<i>Gennada</i> sp./ <i>Natantia</i> sp.	6.38	0.01	0.01	0.00	0.03	0.00
	Sergestidae sp.	6.38	0.01	0.03	0.00	0.00	0.00
	Decapoda larvae	10.64	0.01	0.02	0.00	0.02	0.00
OSTRACODS	<i>Gigantocypris muelleri</i>	21.28	0.10	0.07	0.00	0.30	0.19

901

902 Table 5. Proportion and occurrence of fish species caught during trawl operations. Main contributions
 903 are in bold.
 904

FAMILY	Species	% occurrence	% all stations	% M1	% M2	% M3	% M4
BATHYLAGIDAE	<i>Bathylagus tenuis</i>	23.40	5.52	3.58	0.00	7.94	4.69
GONOSTOMATIDAE	<i>Cyclothone</i> sp. A	25.53	3.18	0.68	0.00	2.65	6.93
	<i>Cyclothone</i> sp. B	2.13	0.06	0.00	0.00	0.13	0.00
STOMIIDAE	<i>Stomias boa/gracilis</i>	21.28	0.83	1.87	0.00	0.97	0.22
ASTRONESTHIDAE	<i>Borostomias antarcticus</i>	2.13	0.03	0.00	0.00	0.06	0.00
IDIACANTHIDAE	<i>Idiacanthus atlanticus</i>	2.13	0.03	0.17	0.00	0.00	0.00
SCOPELARCHIDAE	<i>Bentalbella macropinna</i>	8.51	0.18	0.17	0.00	0.06	0.45
PARALEPIDIDAE	<i>Notolepis coatsi</i>	48.94	3.03	1.70	12.20	1.87	2.46
MYCTOPHIDAE	<i>Electrona antarctica</i>	65.96	27.71	29.64	37.50	17.62	40.22
	<i>Electrona subaspera</i>	2.13	0.03	0.17	0.00	0.00	0.00
	<i>Gymnoscopelus bolini</i>	2.13	0.03	0.00	0.00	0.06	0.00
	<i>Gymnoscopelus braueri</i>	44.68	4.07	3.24	2.68	5.62	2.46
	<i>Gymnoscopelus fraseri</i>	4.26	0.27	0.00	0.60	0.00	0.78
	<i>Gymnoscopelus nicholsi</i>	14.89	0.27	0.17	1.79	0.06	0.11
	<i>Krefftichthys anderssoni</i>	55.32	28.10	20.61	18.15	41.06	14.30
	<i>Krefftichthys anderssoni</i> (postlarvae)	55.32	21.18	32.54	4.17	18.85	24.13
	<i>Nannobrachium achirus</i>	8.51	0.39	0.00	0.00	0.65	0.34
	<i>Protomyctophum andriashevi</i>	4.26	0.12	0.68	0.00	0.00	0.00
	<i>Protomyctophum bolini</i>	38.30	1.54	1.19	6.55	0.19	2.23
	<i>Protomyctophum gemmatum</i>	2.13	0.03	0.17	0.00	0.00	0.00
	<i>Protomyctophum parallelum</i>	4.26	0.06	0.00	0.00	0.13	0.00
	<i>Protomyctophum tenisoni</i>	19.15	0.45	0.85	2.38	0.13	0.00
	Myctophidae (postlarvae)	4.26	0.09	0.00	0.00	0.19	0.00
MURAENOLEPIDAE	<i>Muraenolepis marmoratus</i>	27.66	0.83	0.51	5.95	0.26	0.11
MACROURIDAE	Macrouridae sp.	2.13	0.03	0.00	0.00	0.06	0.00
MELANONIDAE	<i>Melanonus gracilis</i>	4.26	0.12	0.51	0.00	0.06	0.00
MELAMPHAIDAE	<i>Poromitra crassiceps</i>	2.13	0.33	0.00	0.00	0.71	0.00
LIPARIDAE	<i>Paraliparis thalassobathyalis</i>	2.13	0.03	0.00	0.00	0.06	0.00
NOTOTHENIIDAE	<i>Notothenia rossii</i> (blue fingerling)	10.64	0.18	0.00	0.89	0.19	0.00
	Postlarvae type A	25.53	0.95	1.53	6.55	0.06	0.00
GEMPYLIDAE	<i>Paradiplospinus gracilis</i>	4.26	0.06	0.00	0.60	0.00	0.00
ACHIROPSETTIDAE	<i>Achiropsetta tricholepis</i>	6.38	0.12	0.00	0.00	0.26	0.00
	Larvae (unidentified)	6.38	0.18	0.00	0.00	0.06	0.56

905

906 Table 6. Comparison of respiratory carbon fluxes ($\text{mg C m}^{-2} \text{d}^{-1}$) estimated in this study and in other
 907 sites.

908

909

Source	Location	Site	Migrant biomass ($\text{mg C m}^{-2} \text{d}^{-1}$)	Respiratory flux at 2°C ($\text{mg C m}^{-2} \text{d}^{-1}$)
This study ^{a,b}	Kerguelen Islands	Station M1	14,676	0,043
		Station M2	1.761 (0.041 - 5.987)	0.004 (0.000 - 0.012)
		Station M3	1.255 (0.201 - 2.309)	0.005 (0.001 - 0.008)
		station M4	10.072 (5.067 - 15.077)	0.031 (0.016 - 0.045)
Kwong et al. (2020) ^{a,b}	Southeast Australia	Cold core eddy "B-CCE"	0,5	0,17
		Warm core eddy "R-WCE"	4,1	0,56
		Warm core eddy "WCE"	10,6	2,75
Belcher et al. (2019) ^{a,c}	Scotia Sea	JR 161 WSS	49,8	0,05
		JR161 NSS	520,6	0,28
		JR177 GB	238,5	0,13
		JR177 MSS	407,1	0,33
Ariza et al. (2015) ^{a,d}	Canary Islands	North of Gran Canaria	168	0,69
Hudson et al. (2014) ^{a,d}	North Azores	Reykjanes Rdige	5,2	0.003-0.014
		Azorean Zone	40	0.012-0.071
Hidaka et al. (2001) ^{a,b}	Western equatorial Pacific	Station 15	462,5	0,73
		Station 16	248,9	0,39
		Station 8	539,5	0,86
		Station 10	406,5	0,64
		Station 13	726,92	1,1

^aUncorrected for capture efficiency

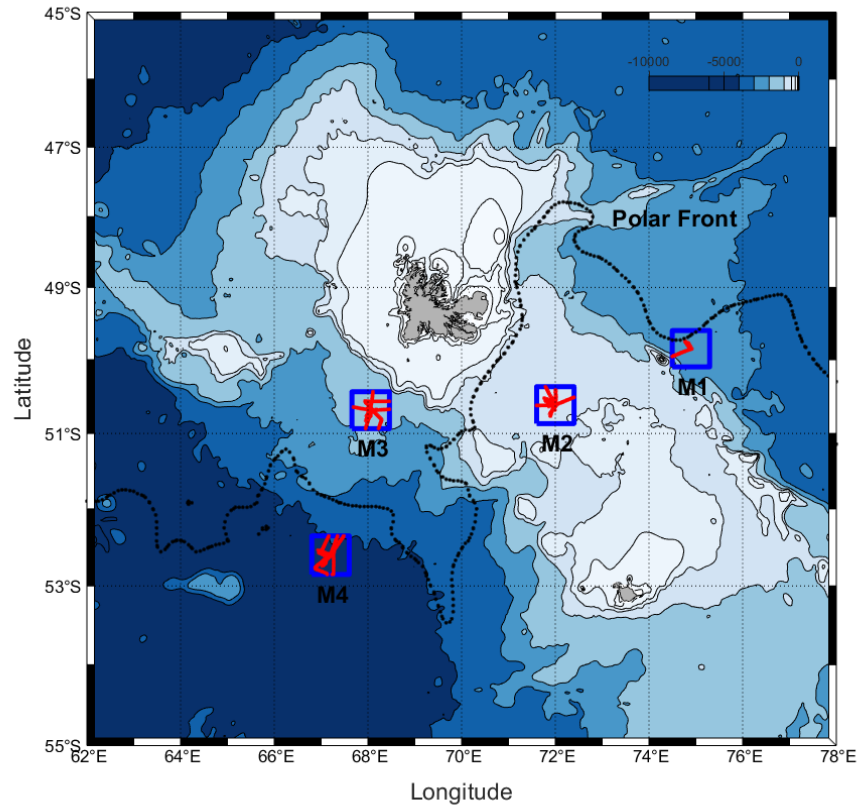
^bAssumes 14% of capture efficiency

^cSmall framed trawl

^dMedium framed trawl

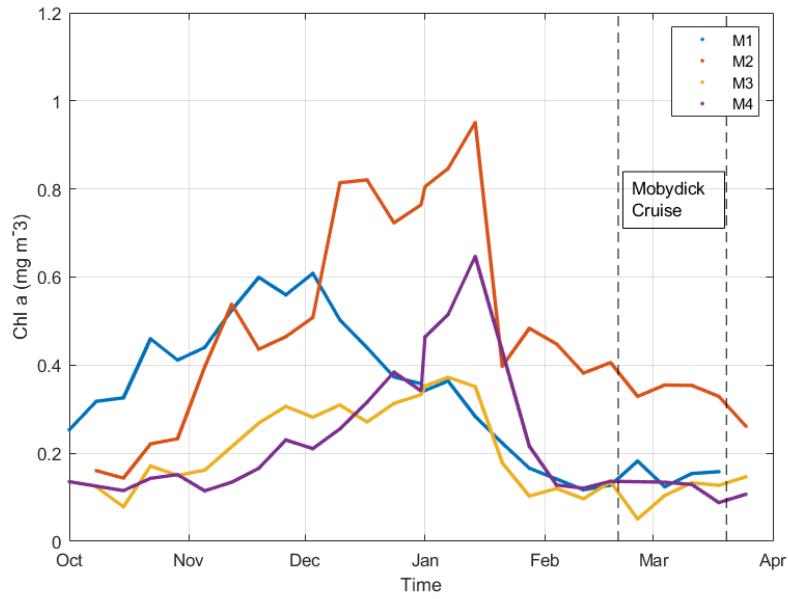
^eLarge pelagic trawl

910 Fig. 1. Locations of the four stations (M1, M2, M3 and M4) in the Kerguelen region during the
911 MOBYDICK survey. Acoustic and trawl data areas are indicated by blue squares. The dotted line
912 indicates the mean location of the Polar Front during the study period.



913
914
915

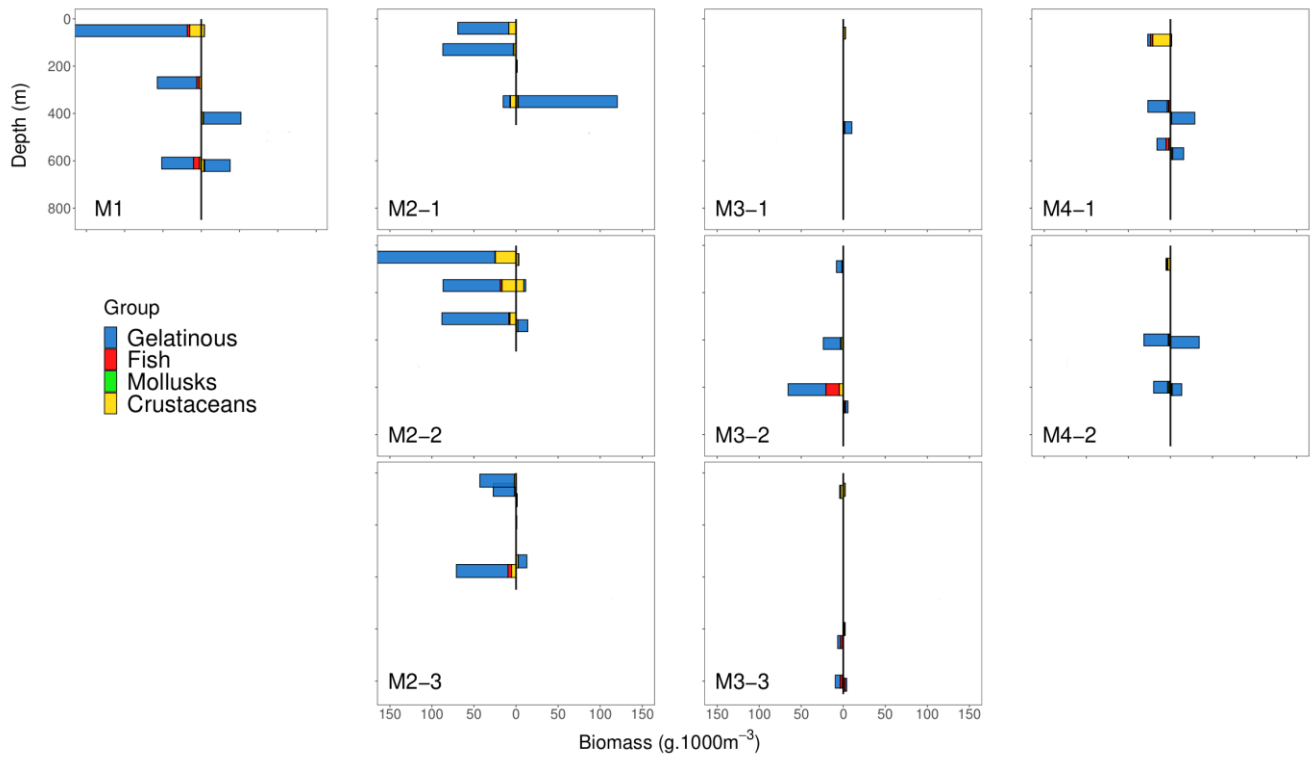
916 Fig. 2. Time series of weekly-averaged chlorophyll a concentration ($\text{mg} \cdot \text{m}^{-3}$) at each MOBYDICK
917 station (blue squares in Figure 1) from October 2017 to March 2018.
918



919

920

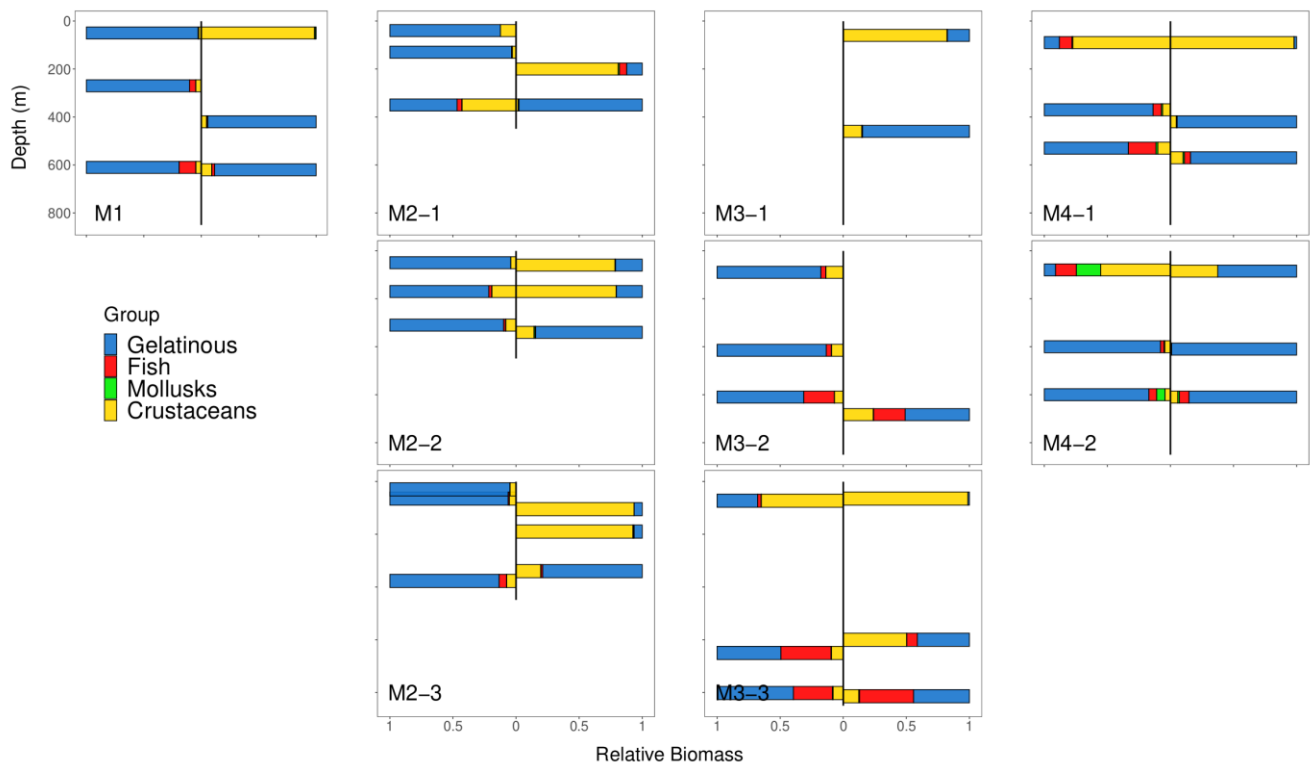
921 Fig. 3. Night-day (left-right) absolute biomass (in $g \cdot 1000m^{-3}$) of macrozooplankton-micronekton from
922 trawls.
923



924
925

926 Fig. 4. Night-day (left-right) relative biomass of macrozooplankton-micronekton from trawls.

927

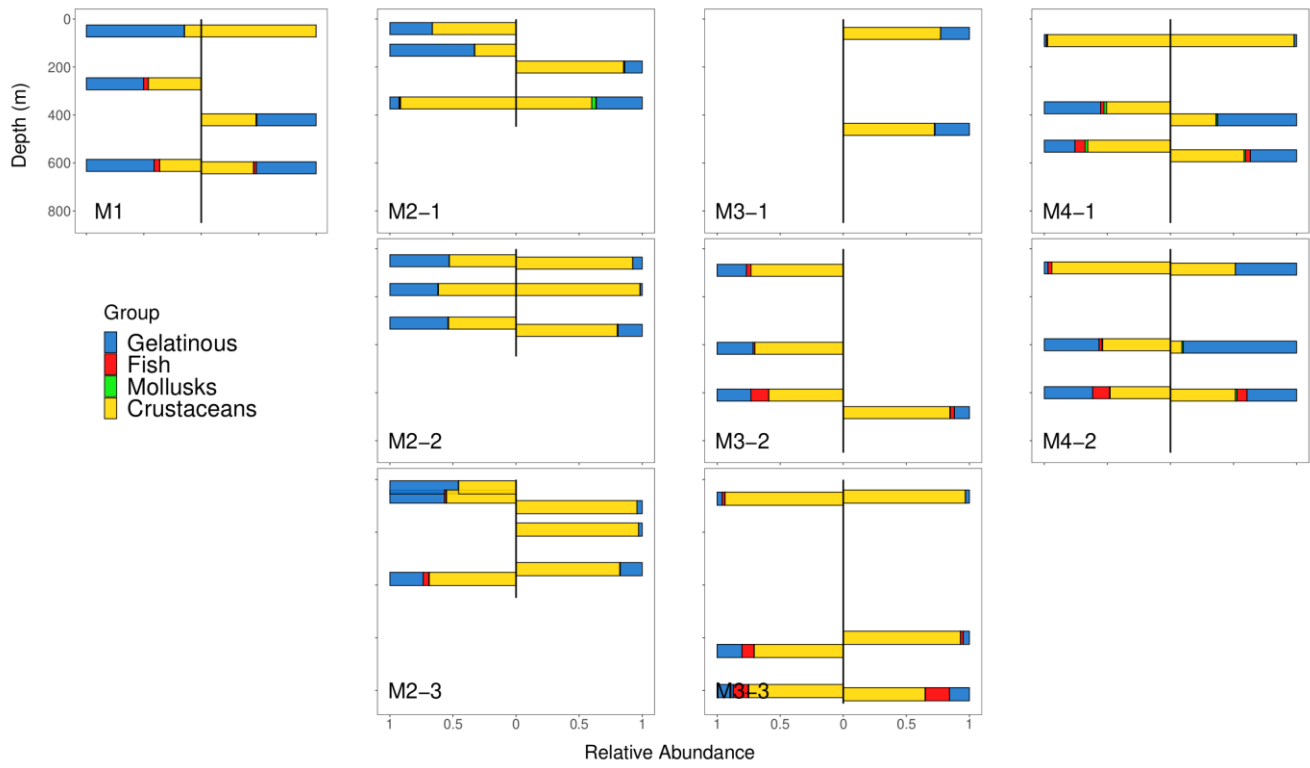


928

929

930 Fig. 5. Night-day (left-right) relative abundance of macrozooplankton-micronekton from trawls.

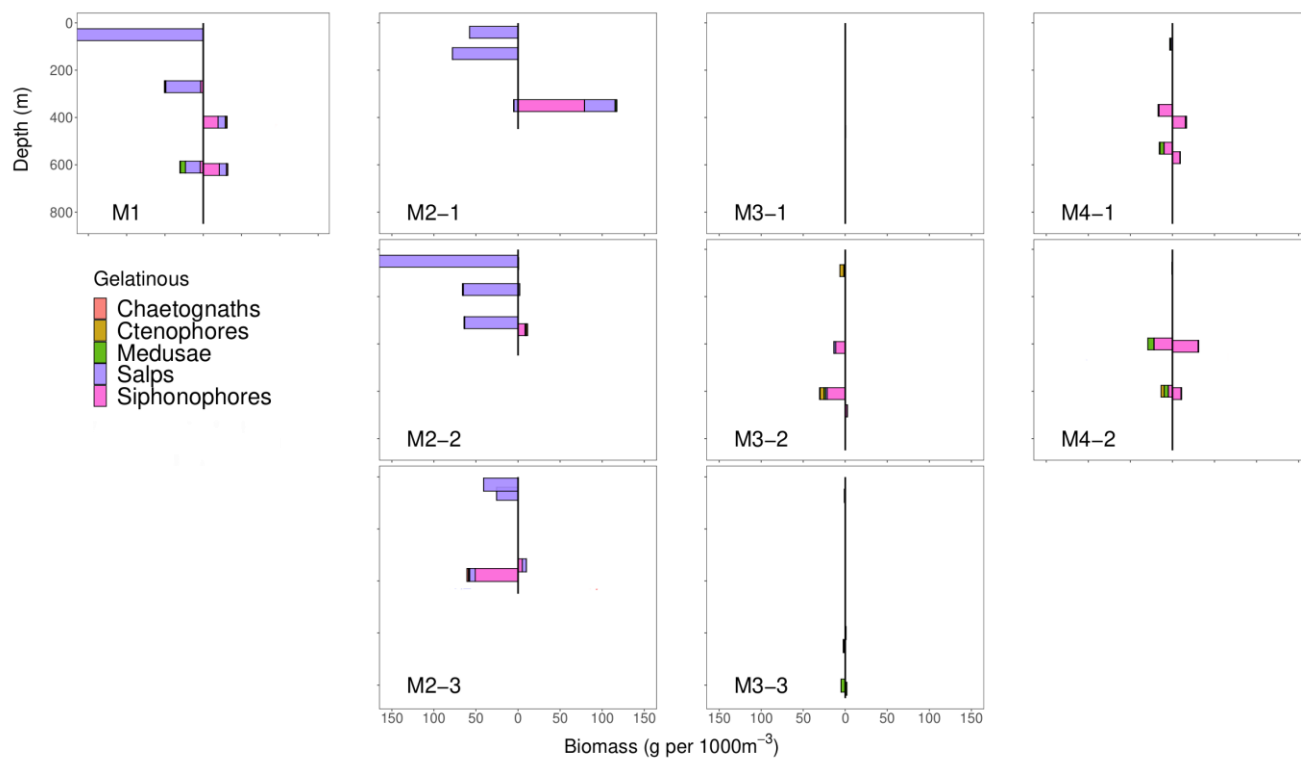
931



932

933

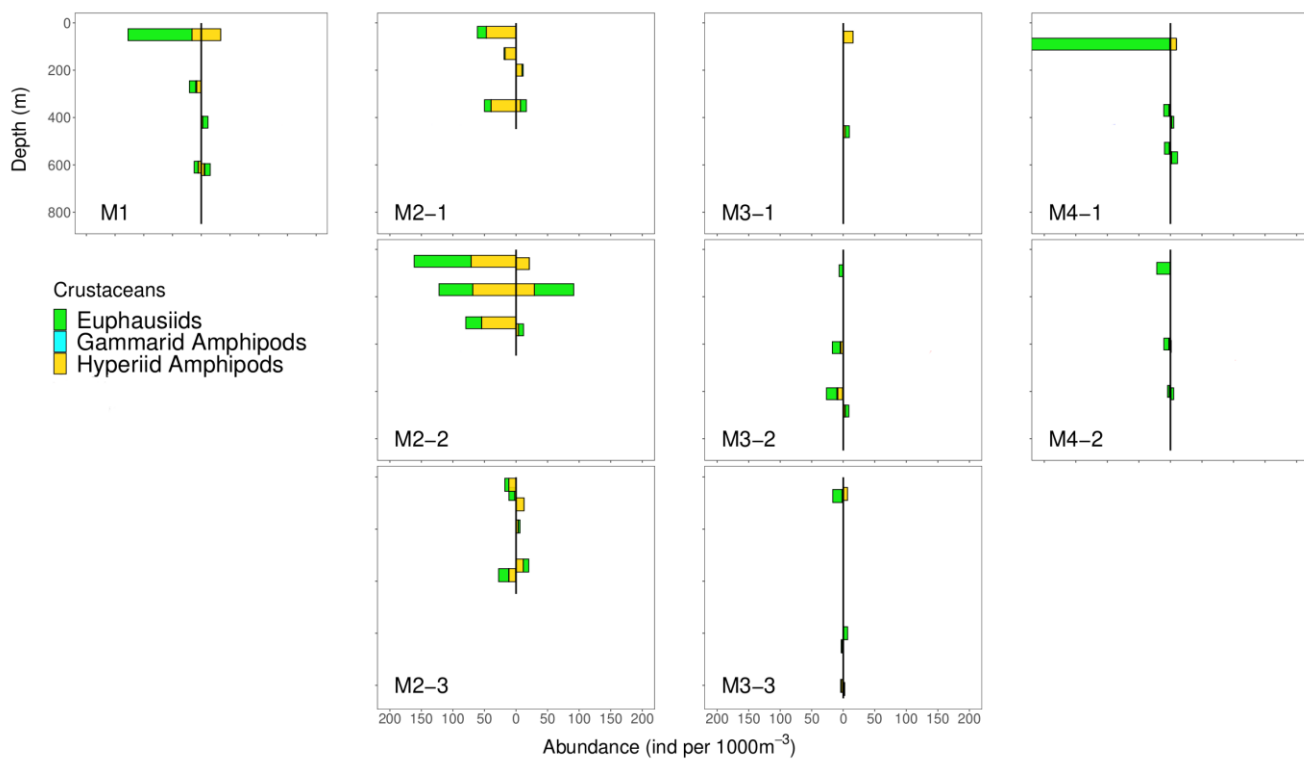
934 Fig. 6. Night-day (left-right) absolute biomass (in $\text{g} \cdot 1000\text{m}^{-3}$) of the main gelatinous organisms from
935 trawls.
936



937

938

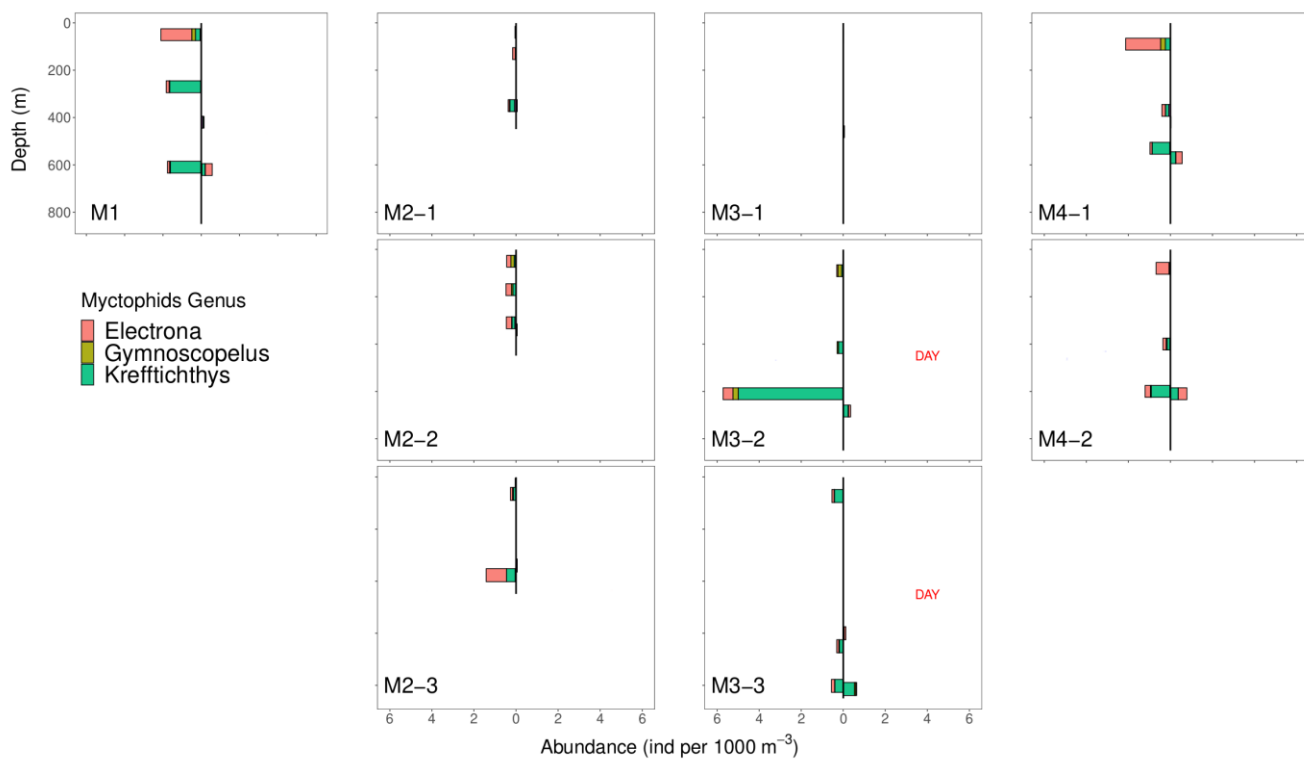
939 Fig. 7. Night-day (left-right) absolute abundance (in individual · 1000m⁻³) of the main crustaceans from
940 trawls.
941



942

943

944 Fig. 8. Night-day (left-right) absolute abundance (in individual · 1000m⁻³) of the main myctophids from
945 trawls.
946

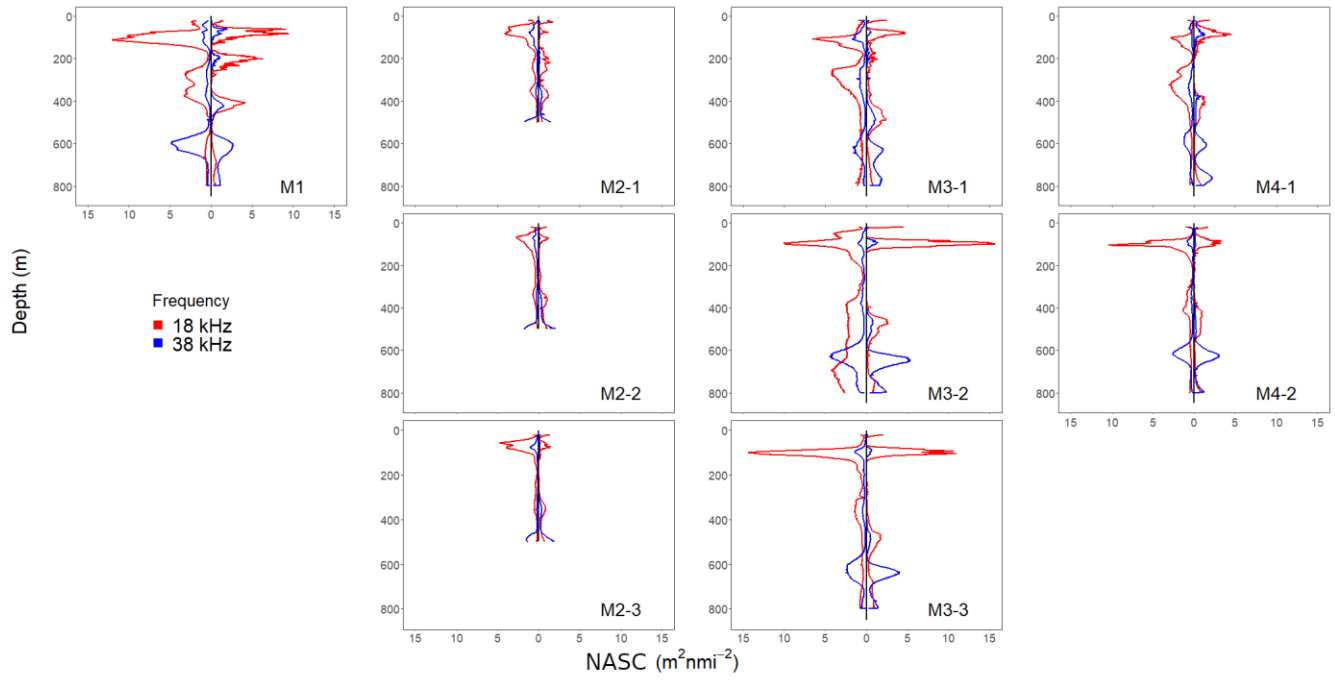


947

948

949 Fig. 9. Night-day (left-right) mean vertical NASC profiles at 18kHz (red) and 38 kHz (blue).

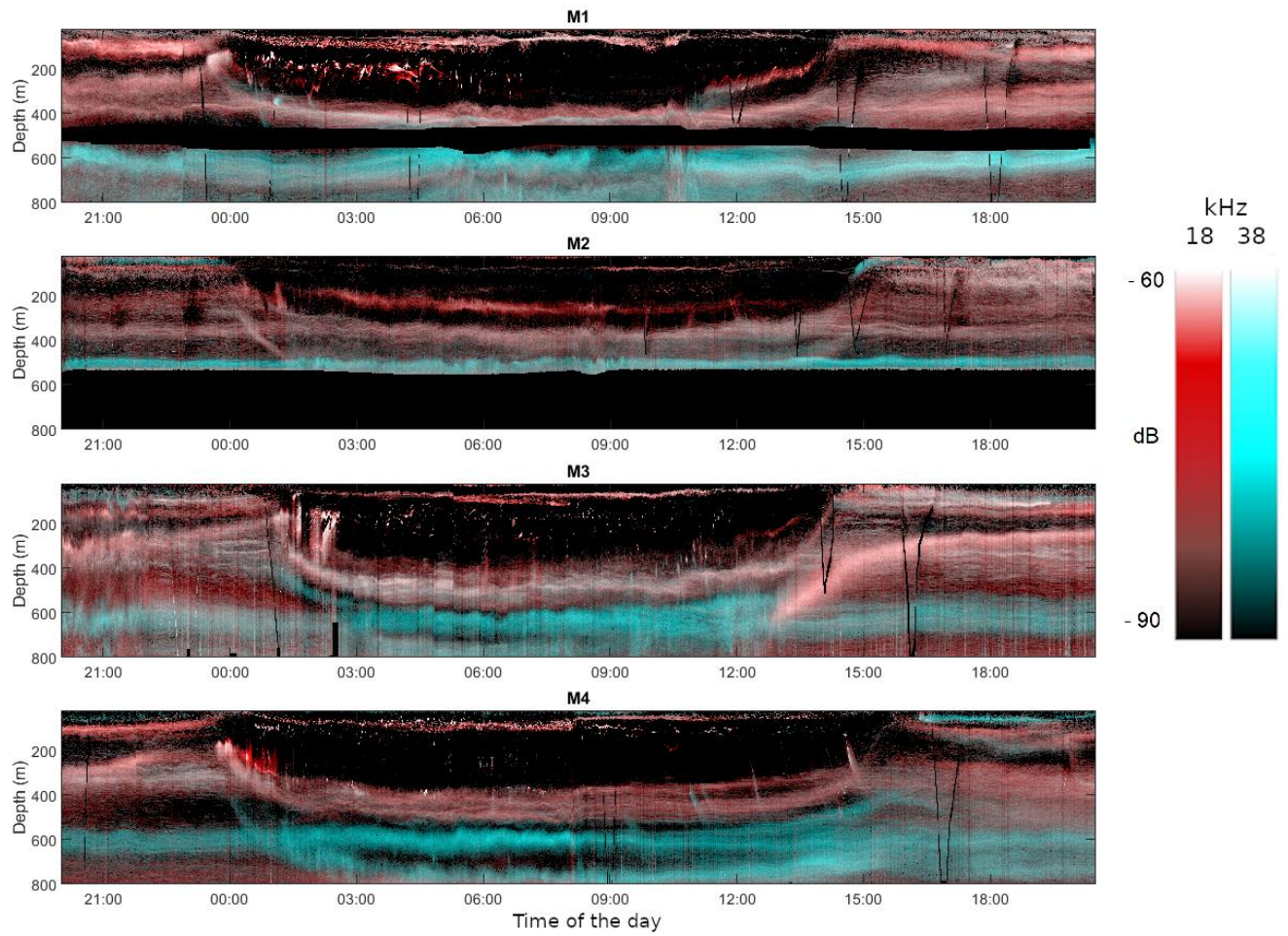
950



951

952

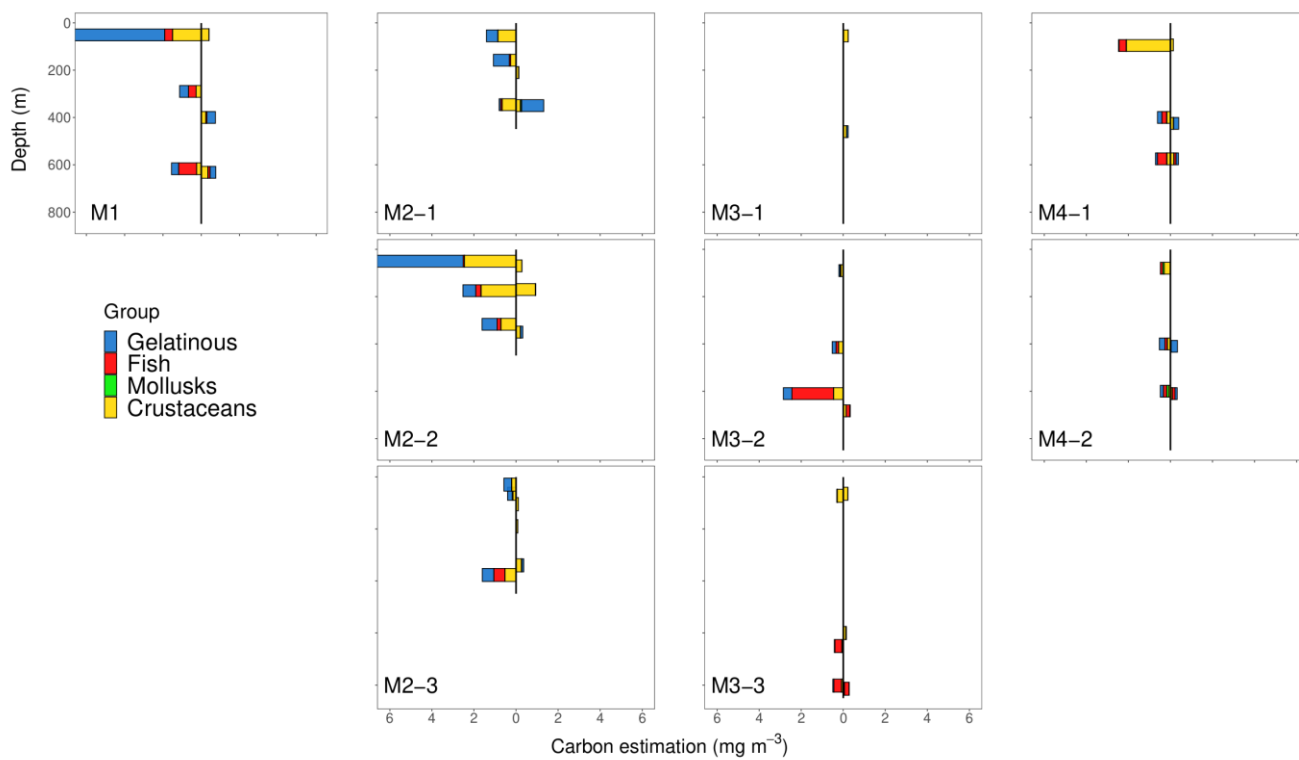
953 Fig. 10. Daily RGB composites of Sv values (dB re · 1m⁻¹) from 12 to 800m for the four stations, with
954 the 18 kHz displayed in red and the 38 kHz frequency displayed both in green and blue.
955



956

957

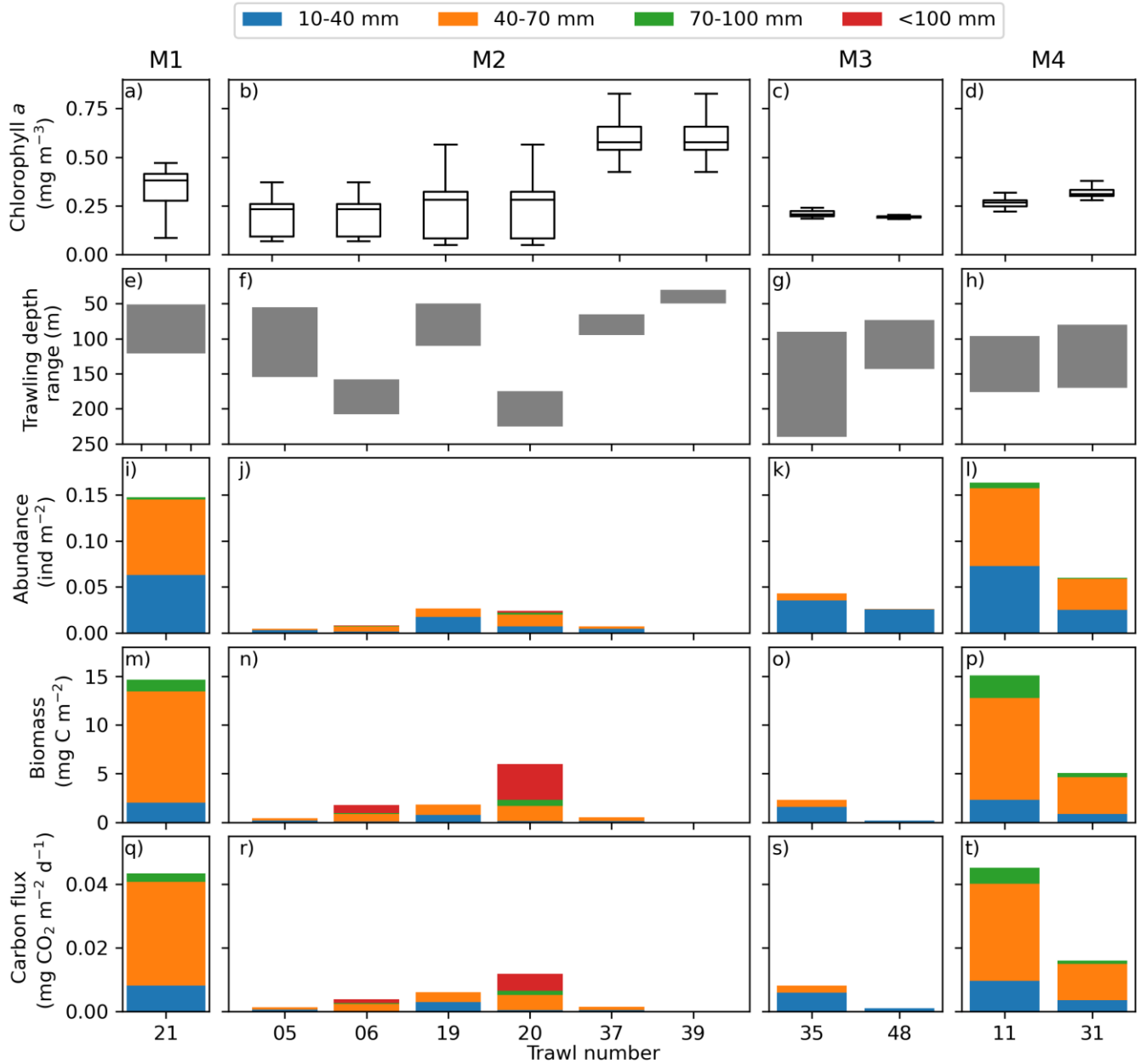
958 Fig. 11. Night-day (left-right) carbon content (in $\text{mg} \cdot \text{m}^{-3}$) of macrozooplankton-micronekton from
959 trawls.
960



961

962

963 Fig. 12. Averaged chlorophyll *a* from 20 to 100 m depth (a-d), depth range of trawling used to target
 964 the migrant layers at each visit (e-h), and migrant abundance (i-j), biomass (m-p) and respiratory
 965 carbon flux (q-t) mediated by fish from the family Myctophidae.
 966



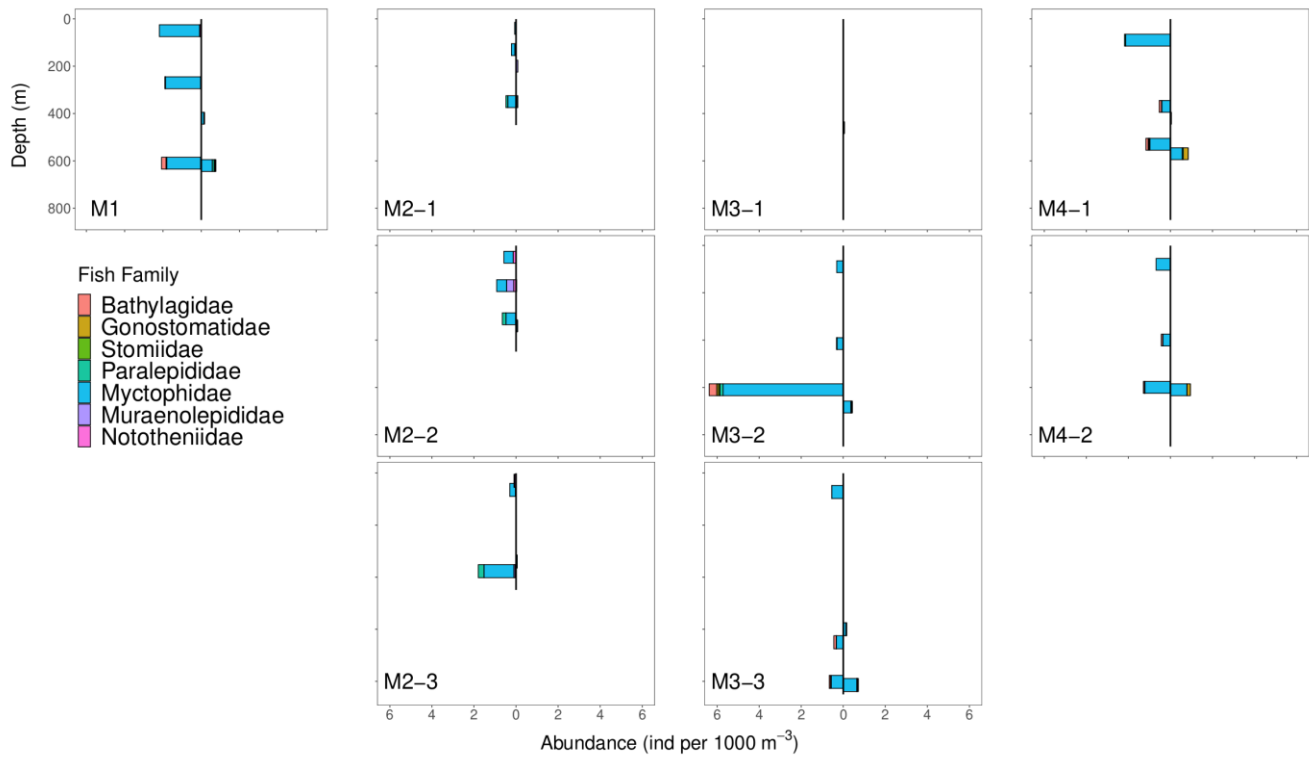
967

968

969 Supplementary material 1

970 Night-day (left-right) absolute abundance (in individual · 1000m⁻³) of fish from trawls.

971



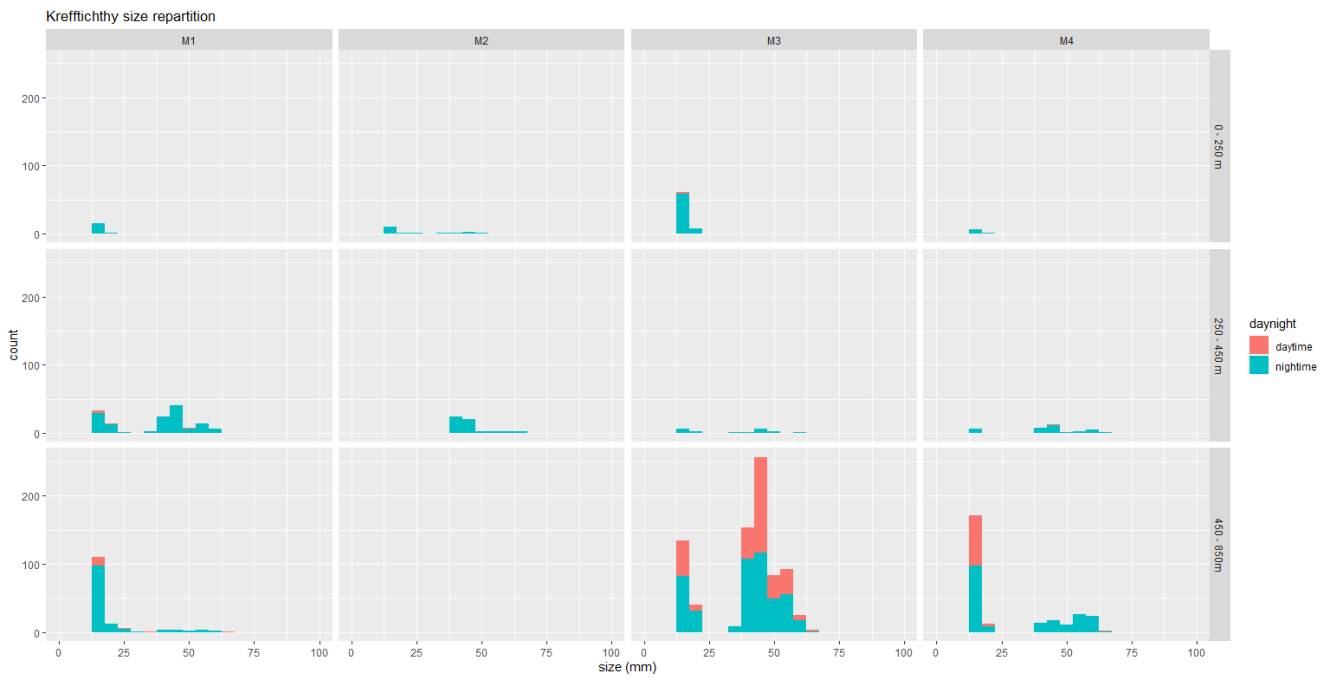
972

973

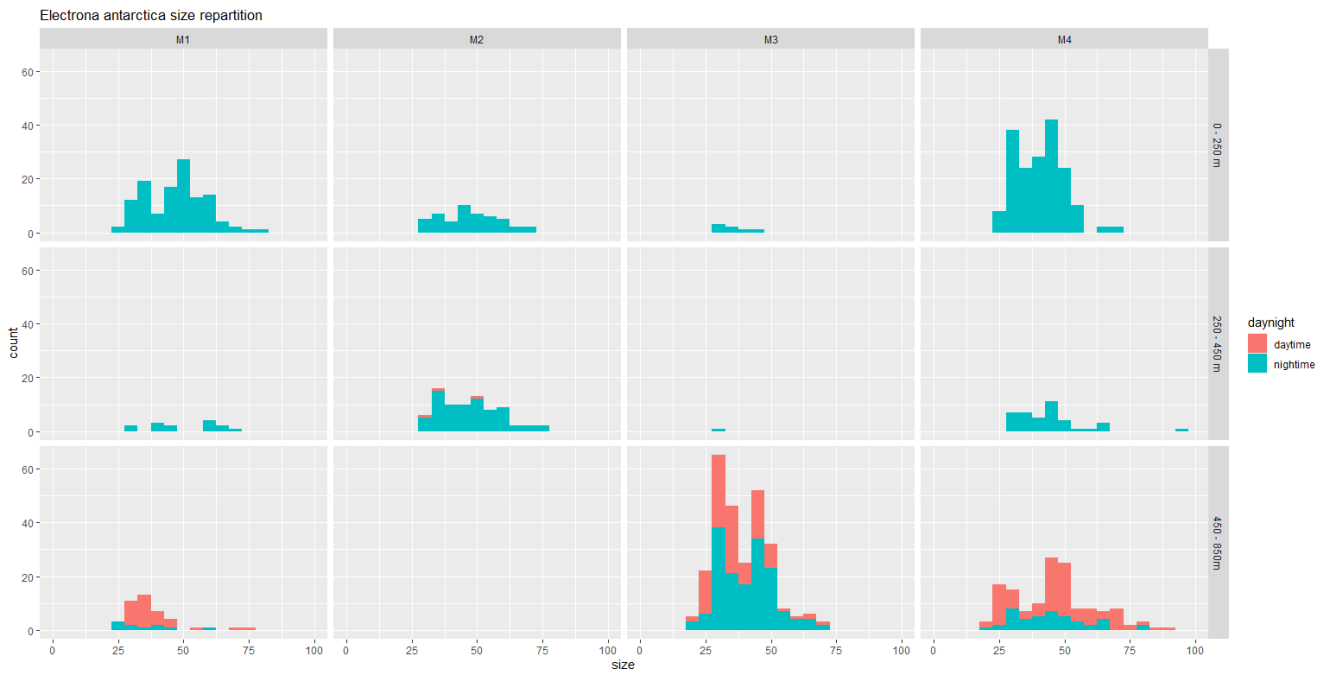
974 Supplementary material 2

975 Size frequency densities for the two main fish species per station and depth strata.

976



977



978

979